EFFECT OF COPPER CONTENT ON THE WEAR, CORROSION AND ANTIBACTERIAL PROPERTIES OF Ti-Nb ALLOYS

2023
MASTER THESIS
METALLURGICAL AND MATERIALS ENGINEERING

Mohammed Riyadh Abdulameer ALAAWAD

Thesis Advisors
Assoc.Prof.Dr. Hüseyin DEMİRTAŞ
Prof.Dr. Rana Afif ANAEE

EFFECT OF COPPER CONTENT ON THE WEAR, CORROSION AND ANTIBACTERIAL PROPERTIES OF Ti-Nb ALLOYS

Mohammed Riyadh Abdulameer ALAAWAD

Thesis Advisors

Assoc.Prof.Dr. Hüseyin DEMİRTAŞ

Prof.Dr. Rana Afif ANAEE

T.C.
Karabük Üniversitesi
Institute of Graduate Programs
Department of Metallurgical and Materials Engineering
Master Thesis
Prepared as

KARABÜK
January 2023

I certify that in my opinion the thesis submitted by Mohammed Riyadh Abdulameer ALAAWAD titled "EFFECT OF COPPER CONTENT ON THE WEAR, CORROSION AND ANTIBACTERIAL PROPERTIES OF Ti-Nb ALLOYS" is fully adequate in scope and in quality as a thesis for the degree of Master of Science

Assoc. Prof. Dr. Hüseyin DEMİRTAŞ .....
Thesis Advisor, Department of Metallurgical and Materials Engineering

Prof. Dr. Rana Afıf ANAEE (UOT) .....
Co-Thesis Advisor, Department of Metallurgical and Materials Engineering

This thesis is accepted by the examining committee with a unanimous vote in the Department of Metallurgical and Materials Engineering as a Master of Science thesis. January 17, 2023

Examining Committee Members (Institutions) Signature

Chairman: Assist. Prof. Dr. Alper İNCESU (KBU) .....

Member : Assoc. Prof. Dr. Yüksel AKINAY (YYU) .....

Member : Assoc. Prof. Dr. Hüseyin DEMİRTAŞ (KBU) .....

The degree of Master of Science by the thesis submitted is approved by the Administrative Board of the Institute of Graduate Programs, Karabuk University.

Prof. Dr. Müslüm KUZU .....
Lisansüstü Eğitim Enstitüsü Müdürü

"I declare that all the information within this thesis has been gathered and presented in accordance with academic regulations and ethical principles and I have according to the requirements of these regulations and principles cited all those which do not originate in this work as well."

Mohammed Riyadh Abdulameer ALAAWAD

ÖZET

Yüksek Lisans Tezi

Ti-Nb ALAŞIMLARINDA BAKIR İÇERİĞİNİN AŞINMA KOROZYON VE ANTİBAKTERİYEL ÖZELLİKLERE ETKİSİ

Mohammed Riyadh Abdulameer ALAAWAD

Karabük Üniversitesi
Fen Bilimleri Enstitüsü
Metalurji ve Malzeme Mühendisliği

Tez Danışmanı:
Doç. Dr. Hüseyin DEMİRTAŞ
Prof.Dr. Rana Afif ANAEE
Ocak 2023, 74 sayfa

Titanyum ve alaşımları, düşük yoğunluk, yüksek mekanik dayanım, yüksek korozyon direnci ve iyi biyouyumluluk gibi mekanik, fiziksel ve kimyasal özelliklerin birleşiminden dolayı çok çeşitli biyomedikal uygulamalara sahiptir. Bu araştırma sırasında, dört farklı ağırlık yüzdesinde Cu (ağırlıkça %0, 5, 7 ve 9) ile toz metalürjisi yöntemiyle dört alaşım (Ti-18Nb-xCu) hazırlandı ve korozyon davranışları, aşınmaya karşı dirençleri ve antibakteriyel özellikleri araştırıldı.

Biyouyumlu malzemeler, metal tozlarının karıştırılması, sıkıştırılması ve daha sonra sinterlenmesiyle oluşturulmuştur. Bu ürünü tıp alanında kullanıma uygun hale getirmek için titanyum (Ti), niyobyum (Nb) ve bakır tozlarının (Cu) bir kombinasyonu kullanıldı. Halihazırda sıkıştırılmış ve sinterlenmiş malzemenin özelliklerini belirlemek için testler yapıldı ve nihai amaç bu malzemenin vücuda yerleştirilebilir tıbbi cihazlarda kullanılmasıydı. Metalik toz karışımının iki zımba ve bir açık kalıpla donatılmış bir hidrolik preste sıkıştırılması sonucunda ham yoğunlukta numuneler

üretildi. Bir sonraki adımda, sıkıştırıldıktan sonra her numune grubu uygun sıcaklıkta sıcaklık kontrollü fırında sinterlendi.

Cu içeriği yüzde 7 veya daha yüksek olduğunda oluşan sert Ti_2Cu fazı sayesinde Ti-18Nb-7Cu alaşımının en düşük aşınma oranına sahip olduğu ortaya çıkmıştır. Üretim aşamasında oluşan katodik ve anodik bölgelerdeki değişimlerin neden olduğu farklı korozyon davranışı nedeniyle alaşım yüzeyinde mikro galvanik hücreler daha kolay oluşmuştur. %7 Cu içeren Ti alaşımının atomik kuvvet mikroskobu (AFM) analizinden elde edilen sonuçlara göre, yüzey pürüzlülüğü en yüksek seviyededir.

Bu tezin bulguları, hücrelere ve bakterilere yakın Cu kullanımının, dokuya zarar vermeyen antibakteriyel malzemeler geliştirmek için malzeme tasarımına doza bağlı bir yaklaşım gerektirdiğini göstermektedir. Çeşitli alaşımlar, kullanım amaçlarına uygun antibakteriyel özelliklere ve mekanik ve korozyon özelliklerine sahip olacak şekilde tasarlanabilir. Bu alanda daha fazla gelişme ile antibakteriyel titanyum alaşımları hem implant endüstrisine hem de yardım etmeyi amaçladıkları hastalara fayda sağlayabilir.

Anahtar Sözcükler : Ti alaşımı, Biyomalzeme, Toz metalurjisi, Korozyon, Aşınma direnci, Antibakteriyel.

Bilim Kodu : 91501

ABSTRACT

Master Thesis

EFFECT OF COPPER CONTENT ON THE WEAR, CORROSION AND ANTIBACTERIAL PROPERTIES OF Ti-Nb ALLOYS

Mohammed Riyadh Abdulameer ALAAWAD

Karabük University
Institute of Graduate Programs
The Department of Metallurgical and Materials Engineering

Thesis Advisors:
Assoc.Prof.Dr. Hüseyin DEMİRTAŞ
Prof.Dr. Rana Afif ANAEE
January 2023, 74 pages

Titanium and its alloys have various biomedical applications due to the combination of mechanical, physical, and chemical properties such as low density, high mechanical strength, high corrosion resistance, and good biocompatibility. During this research, four alloys (Ti-18Nb-xCu) were prepared by powder metallurgy with four different weight percent Cu (0, 5, 7, and 9 weight percent), and their corrosion behaviour, wear resistance, and antibacterial properties were investigated.

Biocompatible materials were created by mixing metal powders, compacting them, and then sintering them. It took a combination of titanium (Ti), niobium (Nb), and copper powders (Cu) to make this product suitable for use in the medical field. Testing was done to determine the properties of the already compacted and sintered material, with the ultimate goal of using this material in implantable medical devices. There is something called green compacted as the result of compacting the metallic powder mixture in a hydraulic press equipped with two punches and an open die. The next step

was to sinter the materials in the temperature-controlled furnace at the appropriate temperature for each group of specimens after they had already been compacted.

It turns out that Ti-18Nb-7Cu alloy has the lowest wear rate thanks to the hard Ti_2Cu phase, which forms most frequently when Cu content is 7 percent or higher. Micro-galvanic cells formed more readily on the alloy surface due to the different corrosion behavior caused by variations in the cathodic and anodic sites formed during the formation phase. According to results from an Atomic force microscopy (AFM) analysis of Ti alloy with 7 % Cu, surface roughness was greatest.

This thesis's findings show that using Cu close to cells and bacteria necessitates a dose-dependent approach to material design to develop antibacterial materials that do not harm tissue. Various alloys can be designed to have antibacterial properties and mechanical and corrosion properties appropriate for their intended use. With further development in this area, antibacterial titanium alloys could benefit both the implant industry and the patients they are intended to help.

Key Word **:** Ti alloy, Biomaterial, Powder metallurgy, Corrosion, Wear resistance, Antibacterial.

Science Code : 91501

ACKNOWLEDGMENT

First, thanks to Allah, who knows everything, rules everything, and sees everything, for granting me this victory and desire to achieve this study.

I would especially like to express my deep appreciation and sincere gratitude to my supervisor's Assoc. Prof. Dr. Hüseyin DEMİRTAŞ and Prof.Dr. Rana Afif ANAEE for their patience, attention, understanding, and balance in carrying out the activities throughout the entire work, accompanying, instructing, and teaching at every step, with total dedication.

In advance, I would like to thank the examining committee members for being willing to collaborate decisively with this work. To my parents for all their dedication in life. To my wife, family, and my friends for their solicitude at all times

CONTENTS

Page

LIST OF FIGURES

Page

LIST OF TABLES

Page

SYMBOLS AND ABBREVIATIONS INDEX

SYMBOLS

α : Alpha

β : Beta

P : Density

E : Young's modulus

μm : Micrometer

I_{corr} : Corrosion Current Density

E_{corr} : Corrosion Potential

ABBREVIATIONS

P/M : Powder metallurgy

ASTM : American Society for Testing and Materials

JCPDS : Joint Committee for Powder Diffraction Standards

Ra : Average Roughness

EDS : Energy-Dispersive Spectrometry

mpy : Mils per year

ROS : Reactive oxygen species

PART 1

INTRODUCTION

1.1 INTRODUCTION

Titanium is a lightweight material that combines high strength and resistance to corrosion [1]. The material is extensively employed in mission-critical applications ranging from aircraft to power production and medical implants. Titanium is used mainly in medical items such as load-bearing orthopedic implants, dental screws, and abutments. $Ti-6Al-4V$ and $CP-Ti$ are two of the most common titanium alloys used in implantable implants today. Today, these metals are quite common in the implant sector. These alloys are so popular because the substance prefers to merge with the surrounding bone in vivo. Branemark et al. [2] created the term "osseointegration" to refer to the formation of the bone surrounding titanium implants. Since this seminal study demonstrated the feasibility of employing commercially pure titanium in implants, numerous other titanium alloys have been proposed for implant operation [3-5].

As a result, titanium alloys have become more prevalent in aviation, aerospace, chemical, shipbuilding, medical, and other industries. Titanium, having a density of 4.5 g/cm^3, is only 60% the density of iron. Titanium alloy materials are being studied, developed, and supported by practical applications across several nations due to the widespread recognition of the relevance of titanium alloy materials [6].

These titanium alloys, a permanent load-bearing implant material, have been demonstrated to fulfill essential human locomotor and mastication functions. While these materials are critical for current treatments, they are not without drawbacks. The particular concerns include, but are not limited to, "stress-shielding" owing to the implant's high Young's Modulus (in contrast to bone) and bacterial infections of the surrounding tissue [6]. Concerning germs, these materials and any surface in a clinical context are susceptible to contamination by bacteria, particularly the prevalent Staphylococci type [7]. While these bacteria are not necessarily dangerous and are abundant in the human body as common environmental organisms, the antibiotic-

resistant strains of these bacteria are a severe worry that may result in mortality in certain situations [7]. Staphylococcus epidermidis (S.E.) and Staphylococcus aureus (S.A.) are implicated strains. S.A. is a crucial worry because of its antibiotic-resistant strain, but the virulence and gene alterations described for S.E. may provide an additional hazard to healthcare shortly [8]. Thus, these bacteria are unwanted in the clinical environment and burden the healthcare system. This is because infections caused by some strains of bacteria might aggravate pre-existing medical issues. Also, microorganisms may infect sterile titanium implant surfaces during medical implantation.

Bacteria reproduce rapidly after colonizing a surface and being transferred into the human body, which is a nutrient-rich environment. Bacteria's quick growth rate is one of the reasons they are a significant source of worry in healthcare settings because they represent a danger to people. While this risk is associated with contaminated implant surfaces, where bacteria multiply fast in vivo after surgery, this is not the sole source of the bacterial load. Apart from the rapid colonization of surfaces, the bacterial load is exacerbated because many bacteria have gained resistance to drugs over time [8]. Consequently, the current situation in healthcare is one in which typical antibiotics may or may not be used to treat bacterial infections, necessitating the ongoing need for novel antibiotics. For these reasons, there has been an increase in interest in antibacterial materials that do not need antibiotic treatment to address bacterial load. Antibacterial materials are of interest for a variety of reasons. Generally, they involve inducing a bactericidal property into the implant material through a variety of methods, including alloying titanium with silver or copper [9], treating titanium surfaces with surface treatments [10], or coating materials with thin-film coatings [11].

Copper ions were considered to be the key contributor to the antibacterial action. Consequently, preliminary research was conducted to measure the association between copper ions in a fluid and the resulting toxicity and viability of bacteria and cells. This was justified to facilitate the later creation of titanium-niobium-copper alloys with the desired characteristics. Because bacteria contaminate implant surfaces mainly, research was conducted on bacteria in direct contact with titanium-copper surfaces to measure the bactericidal effects of these materials [12].

In addition to using antibiotics during surgery, implants with antibacterial qualities are another way to lower the risk of bacterial infection. When it comes to making implants

with antibacterial surfaces, surface modification has shown to be a successful method. Several techniques, including ion implantation, plasma immersion, magnetron-sputtering, deposition, dipping coating, electroplating, U.V. irradiation, polymer modification, plasma spraying, and oxidation, have been developed to enhance the antibacterial properties of implant devices [13]. Much research has been done on anti-adhesion and antibacterial surfaces that contain incorporated antimicrobials, ions such as F +, Cu, Ag, and Zn, or antiseptics [14]. However, the surface features have a substantial impact on antibacterial activity. Inadequate adhesive strength, for example, is always the reason for poor adhesion of the antibacterial coating of the TiO_2 deposition layer, resulting in the loss of antibacterial properties. Typically, the antibacterial surface of an implant for ion implantation is much thinner than typical. The antibacterial properties of the antibacterial surface will be lost as soon as any cause degrades the antibacterial surface. A metal with antibacterial action throughout the alloy rather than only on the surface is thus an absolute need. Antibacterial stainless steels were created by incorporating Cu or Ag elements into the steel and heating it to the right temperature [14].

The biocompatibility and antibacterial characteristics of copper (Cu), one of the essential trace metals in the human body, have led to its widespread use. Most scientists agree that the Cu ion emitted from surface coatings or alloys is critical to antibacterial coatings and materials' performance. When the Cu concentration ions are high, the antibacterial activity is also high. On the other hand, a high concentration of metal ions might lead to metal allergy [15].

The manufacturing methods of these new alloys constitute a significant issue since most Titanium alloys include several refractory components with high melting temperatures. As a result, it generates heavy weight, difficult melting and solidification processes, and expensive die costs [16].

An alternate technique of manufacturing, powder metallurgy (P/M), involves using metal powders to create a product via a process of compacting and sintering. This technique is often used to fabricate basic, dimensionally stable geometries, work with materials with too high a melting point, or construct components that would be impossible to make by any other means [17].

1.2 OBJECTIVE OF THE WORK

Several studies have been carried out using different compositions and processing methods of the ternary Ti-Nb-Cu alloy. However, the variation in the titanium content and the absence, many times, of the investigation of parameters significantly influence the mechanical properties, electrochemical properties, and anti-bacterial behavior. The following steps can summarize this aim:

- Production of Ti—18Nb alloy by powder metallurgy method
- Investigate the effect on corrosion behavior by adding Cu in different ratios.
- Investigation of the influence of alloying metals in varying proportions on the antibacterial characteristics of Ti matrix.
- Investigations on the influence of various Cu ratios on microstructure.

As a result of these aims, the main target is; to determine the effect of Cu (biocompatible) on the Ti-18Nb matrix's corrosion behavior and antibacterial properties.

PART 2

LITERATURE REVIEW

Due to their high strength-to-weight ratio, low Young's modulus, and biological compatibility, titanium alloys are promising metallic materials for long-term bone implant applications. Researchers focused on modifying the surfaces of these alloys to increase wear resistance and bioactive properties because of their low corrosion and abrasion resistance [18].

In his work, the motivation for the study was two parts. The first motivation concerns the preparation of Ti-18Nb-xCu alloys, where (x= 5, 7, and 9 wt%). The second motivation was the investigation of corrosion properties in simulated human body fluid at 37°C and dry wear at different loads (5, 10, and 15 N).

Yoshimitsu studied the effect of V ions in a culture medium on the microstructure, corrosion resistance, mechanical characteristics, and fatigue parameters of Ti-15Zr-4Nb-4Ta alloy in a physiological saline solution before 2010 [19]. By melting pure elements in an arc melting furnace, heating them to 950°C for one hour under high vacuum, then quenching them in water at room temperature, D.M. Gordin et al. produced the $Ti-12Mo-5Ta$ alloy. X-ray diffraction enabled them to identify a novel alloy and reveal its body-centered cubic structure. Young's modulus and corrosion behavior in Ringer's solution was also measured [20]. In order to determine the importance of the passive layer in protection, R. Godley et al. compared the corrosion behavior of $\beta-Ti-45wt.\%Nb$ ($Ti45Nb$) to that of $Ti6Al4V$ and $Ti-55wt.\%Ni$ ($Ti55Ni$, Nitinol) alloys in Ringers' solution [21]. The electrochemical behavior of a near- Ti-13Nb-13Zr alloy in 0.9 wt% NaCl solution, Hanks' solution, and minimal essential medium (MEM) at 37 °C was investigated by S. L. Assis et al. using open circuit potential measurements, electrochemical impedance spectroscopy (EIS), and polarization curves. The results showed that Ti alloy was inert in all tested electrolytes and that an oxide layer was present; this layer had a duplex structure with a barrier layer on the inside responsible for the alloy's corrosion resistance and a porous

layer on the outside for its osteointegration properties [22]. Using as-cast $Ti-30Nb-Zr$ alloys in a 0.9% NaCl (0.15 mol L) solution at 25 °C and a neutral pH range, Danielle . et al. studied the effects of Zr content (7.5 and 15 wt%) on microstructure and corrosion resistance. According to the findings, stabilizing the β-phase by incorporating Zr into a $Ti-30Nb$ alloy was successful [23]. Using various techniques, BL Wang et al. investigated the impact of Sn on the microstructure, phase composition, and shape memory effect of Ti-16Nb-xSn alloys (x = 4.0, 4.5, and 5.0 at%). They found that the shape recovery ratio decreases while the β- phase in alloys becomes more stable as Sn content rises [24, 25].

While before 2020, In a Ringer's solution, I. Cvijovi et al. investigated the wear and corrosion behavior of cold-rolled $Ti-13Nb-13Zr$ and $Ti-6Al-4V$ alloys. At room temperature, the wear tests were conducted with a constant load of 40 N with sliding speeds of 0.26, 0.5, and 1.0 m/s. In addition, the corrosion behavior was investigated at 37 °C using potentiodynamic polarization and open circuit potential-time measurements. The findings revealed that $Ti-13Nb-13Zr$ alloy has much worse wear resistance than $Ti-6Al-4V$ alloy in both microstructural circumstances [26]. Yong-yuan et al. used consumable vacuum arc melting to create a $\beta-type$ $Ti35Nb2Ta3Zr$ alloy, which they then tested for corrosion resistance and cytotoxicity in Ringer's solution using open circuit potential, electrochemical impedance spectroscopy (EIS), and potentiodynamic polarization techniques. While both $Ti6Al4V$ and Ti had strong corrosion resistance, this alloy outperformed them in biocompatibility [27]. Using artificial saliva at 37°C, Ana Lcia et al. compared the electrochemical behavior of $Ti35Nb5Zr\ and\ Ti35Nb10Zr$ alloys to that of $Ti6Al4V$ alloys, another biomaterial utilized in dentistry. Corrosion potential increased with immersion duration for all alloys, with $Ti35Nb5Zr$ and $Ti6Al4V$ alloys having a smaller proportion of TiO_2 phase than $Ti6Al4V$ exhibiting the most noticeable rise in corrosion potential [28]. Jose Maria et al. investigated a ternary Ti-15Zr-10Nb alloy, noting its new microstructural and mechanical features and remarkable long-term corrosion resistance in simulated physiological fluids. Micrographs taken with scanning electron microscopy (SEM) and optical microscopy revealed the presence of a biphasic + Widmanstatten microstructure, characterized by the recognizable interleaving lamellae of and phases. The alloy has a Young's modulus of 64 GPa, which is very close to human bone, a strain to fracture that of Ti, and an

appropriate ultimate tensile strength of 0.2%. TiO_2, ZrO_2, and Nb_2O_5 passive films are 5.5±0.5 nm thick in their native condition, making this alloy very durable [29]. Hydrothermally synthesized nanoscale TiO2 coatings on $Ti24Nb4\,Zr7.9$ Sn (Ti-2448) surfaces were tested for their cytocompatibility and osseointegration by Liu et al. The osteoblast cell line $MC3T3-E1$ was grown on either nano$TiO_2/Ti-2448\ or\ Ti-2448$, and its proliferation and alkaline phosphatase (ALP) activities were examined. Additionally, nanoTiO_2/Ti-2448 had a rougher surface than Ti-2448; inflammatory cells were discovered near $nanoTiO_2/Ti-2448$; the cytocompatibility and early detection osseointegration were enhanced. [30]. Using phosphate-buffered solution (PBS), PBS with bovine serum albumin (PBS/BSA), and PBS with hyaluronic acid (PBS/HA), Weijiu et al. studied the corrosion behavior and wear of Ti-25Nb-3Mo-3Zr-2Sn alloy in these physiological solutions. Characterization data revealed that TiO_2, ZrO_2, Nb_2O_5, Mo_2O_5, and SnO_3 all form inert, transparent films [31]. The tribocorrosion behavior of $Ti-15Zr-7.5Mo\ and\ Ti-15Zr-15Mo$ alloys was investigated and evaluated against an alumina sphere by D. R. N. Correa and colleagues. The findings indicated that both alloys had behavior that is superior than $cp-Ti$ [32].

The tribocorrosion behavior of $Ti–Cu$ was investigated by Miamian et al., and they compared it to the tribocorrosion behavior of pure Ti. This comparison was made against a silicon nitride sphere to estimate open-circuit potential and coefficient. The findings indicated that $Ti–Cu$ had superior tribocorrosion properties [33]. Electrochemical impedance spectroscopy (EIS) and reciprocating sliding tests using a ball-on-plate tribometer under 1 N load and alumina as J. Urrea and colleagues used counter-material to study the corrosion and tribocorrosion behavior of titanium surfaces that had been modified through thermochemical treatments. Their goal was to determine how much of an impact Nb and Mo have on titanium's corrosion and tribocorrosion properties. According to the findings, the anti-corrosive capabilities of the $Ti-Nb\ and\ Ti-Mo$ surfaces were superior to those of the $CP-Ti$ surfaces. [34]. The characteristics of $Ti-XCu$ alloys (Cu concentration up to 10 wt%) were studied by Lee Fowler et al., who discovered that alloys with above 3 wt% In addition to the two phases present in Cu, the volume percentage of Ti_2Cu increased. Unaged 5 wt% Cu alloys indicated a possible Ti_3Cu phase in addition to the $\beta-Ti$ phase [35].

In 2020, Recent studies by Fabiana et al. examined the wear, corrosion resistance, and tribocorrosion behavior of the ternary alloy $Ti26Zr24Nb$ when exposed to a pH=7, deaerated Hanks solution at 37 °C [36]. Mechanical alloying of elemental powders was followed by spark plasma sintering to create a grain-structured $Ti-34Nb-25Zr$ alloy, which was then subjected to corrosion testing by Mahundla et al. [37]. To improve the physical, chemical, biological, and mechanical characteristics of -Ti alloys and electrochemical treatments, I.Çaha et al. reviewed the various surface functionalization approaches. [38]. In 2021, Jassim et al. developed a powder metallurgy technique ($at\ 950\ °C\ for\ 6\ h$) to create low modulus -type Ti-based alloys with varying amounts of indium (0.5, 1, 1.5, and 2 wt%) for usage in the medical field. X-ray diffraction, scanning electron microscopy, and the measurement of a few mechanical parameters was used in the characterization (Brinell hardness, compression, and elastic modulus). The findings of an investigation into the wear and corrosion behavior of indium particles in Hanks and saliva solutions showed that 2 wt% indium offered superior mechanical and wear characteristics. [39]. Shivaram et al. utilized powder metallurgy (P/M) to produce a porous $Ti-20Nb-5Ag$ alloy, and they investigated the tribocorrosion behavior of the fabricated alloy in simulated body fluid (SBF) under various applied loads ranging from 1 to 10 N using D.C. electrochemical corrosion technique and kinetic parameters [40].

PART 3

THEORETICAL BACKGROUND

3.1 INTRODUCTION

The development of biomaterials proves to be fundamentally important. This development prescribes an improvement in people's standard of living, represented by an increase in life expectancy, general health, and population well-being.

Since 1952, titanium and its alloys have been utilized as structural materials. Due to their high mechanical strength-to-weight ratio and outstanding corrosion resistance, they are highly desirable. However, they have some disadvantages, such as high cost compared to more common metals such as steel. The higher cost is mainly due to the manufacturing process. Given this negative aspect, titanium stands out in some application areas, especially those requiring high technology, such as aerospace, automotive, chemical, and food industries, and biomaterials [18].

The earth's crust is rich in titanium, a transition metal that may be found in several minerals, including rutile and ilmenite. The primary route to obtain titanium is from the Kroll process conceived in the 1930s, which associates $TiCl_4$ with calcium. Due to its mechanical properties and low density compared to other metals, titanium has aroused great industrial interest. Titanium alloys can present mechanical strength similar to steel with a lower density ($4.51\ g/cm^3$). These characteristics make titanium and its alloys widely used in various industrial segments, such as aerospace, power generation, petrochemical, automotive, and medical and dental industries. [41].

At room temperature, pure titanium has a hexagonal compact (H.C.) crystal structure called α. With heating above 883ºC, the structure becomes BCC, called β. Unlike most H.C. metals, titanium can undergo large cold deformations, even above 90%. The explanation for this phenomenon lies in the relationship between the crystal lattice "c" and "a" parameters of the H.C. crystal structure of titanium, which is 1.587. This value is below the theoretical value of 1.633 for compact hexagonal metals, thus facilitating

The occurrence of crystallographic plane slips. Pure magnesium, for example, which has a c/a ratio of 1.624, cannot undergo cold deformation of more than 50% without fracturing [42]. In Figure 3.1, it is possible to observe the allotropic structures of Ti and their respective network parameters

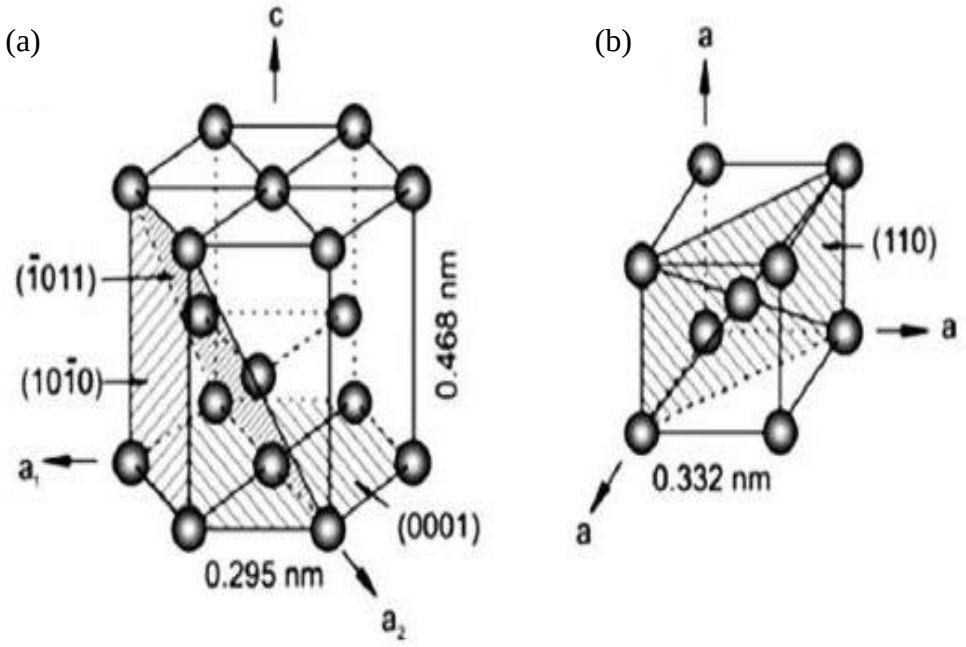

Figure 3.1 Allotropic structures of titanium [42].

Ti and its alloys are classified in grades based on their chemical composition. Based on the percentages of interstitial elements, commercially pure titanium ($cp - Ti$) is classified in grades 1 to 4. The mechanical characteristics of titanium are sensitive to even minute interstitial changes.

In general, alloying elements added to titanium can be classified according to their influence on the allotropic transformation. Alloy elements that change the transition temperature from α-phase to β-phase are classified as β-stabilizers (downward) or α −stabilizers (upward). Also, alloying elements that promote eutectoid transformation are called $\beta - eutectoid$ stabilizers. Based on the microstructure at room temperature, alloys are classified as $\alpha - titanium$ $(or\ quasi - \alpha)$, $\beta - titanium$ $(or\ quasi - \beta)$, and titanium$-(\alpha + \beta)$ [43].

α-titanium alloys have properties observed in other HC-structured alloys. They do not present, for example, sensitivity to the ductile-fragile transition and can be used at low temperatures. They do not respond significantly to heat treatments, have high yield strength, good mechanical strength even at high temperatures, and high modulus of elasticity [43].

As mentioned before, the β-stabilizing alloying elements, when added in large amounts, significantly decrease the allotropic transformation temperature, allowing the BCC phase of titanium to become metastable or even stable at room temperature. This type of alloy is susceptible to heat treatments, and several types of research have been developed to analyze these alloys' mechanical properties and microstructure after different treatments [44]. Due to their low modulus of elasticity, β −titanium alloys are intensely interested in medical and dental applications. One of the disadvantages of using metallic materials as implants is the difference in the modulus of elasticity between the alloy and the bone tissue. The more significant the difference between the elasticity modulus, the greater the possibility of generating a phenomenon called stress shielding, which induces local bone resorption and compromises the functioning of the prosthesis [18]. This and other aspects will be discussed in more detail in later sections. Titanium alloys $(\alpha + \beta)$ combine good mechanical properties with an excellent balance of the characteristics of the $\alpha\ and\ \beta$ phases. These alloys respond significantly to heat treatments that generate a great possibility of combinations of microstructures and different mechanical properties. Although they do not have a fracture strength limit of the same magnitude as α-titanium alloys, they do not have the disadvantages of these alloys and have more excellent ductility and workability.

The primary titanium alloy (α + β) is the $Ti - 6Al - 4V$ alloy. This alloy was initially developed for the aerospace industry but is applied in the automotive industry and with changes in chemical composition, such as medical and dental implants [45]. Due to its great commercial importance, this alloy, along with cp-Ti grade 4, will be used to compare other alloys throughout the work. Table 3.1 presents some mechanical properties and comparisons between $\alpha, \beta, and\ \alpha + \beta$ alloys.

Table 3.1 Properties of Ti alloys [45].

Phase	Materials	$\sigma r\ (MPa)$	$\sigma e\ (MPa)$	ε (%)	$E\ (GPa)$
α	$Ti\ grade\ 1$	240	170	24	102,7
	$Ti\ grade\ 2$	345	275	20	102,7
	$Ti\ grade\ 3$	450	380	18	103,4
	$Ti\ grade\ 4$	550	485	15	104,1
β	$Ti-6Al-4V$	$895-930$	$825-869$	$6-10$	$110-114$
	$Ti-6Al-4V\ ELI$	$860-965$	$795-875$	$6-10$	$101-110$
	$Ti-6Al-7Nb$	$900-1050$	$880-950$	$8.1-15$	114
	$Ti-5Al-2{,}5Fe$	1020	895	15	112
α +β	$Ti-13Nb-13Zr$	973-1037	836-908	10-16	79-84
	$Ti-12Mo-6Zr-2Fe$	1060-1100	1000-1060	18-22	74-85
	$Ti-15Mo$	874	544	21	78
	$Ti-15Mo-5Zr-3Al$	852-1100	838-1060	18-25	80
	$Ti-15Mo-2.8Nb-0{,}2Si$	979-999	945-987	16-18	83
	$Ti-35.3Nb-5.1Ta-7{,}1Zr$	596,7	547,1	19	55
	$Ti-29Nb-13Ta-4{,}6Zr$	911	864	13,2	80

The following topics will address cp-Ti and alloys' mechanical, microstructural, and biocompatibility characteristics. More focus will be given to β-type alloys, especially Ti-Nb However, other widely used alloys, such as Ti-6Al-4V, Nitinol, and other β-type alloys, will also be addressed in the literature review for comparison, contextualization, and verification of the current state of the art.

3.2 STABILITY OF PHASES IN ITS ALLOYS

Developing Ti alloys for biomedical applications and good mechanical properties has focused part of its attention on improving Ti-XNb alloy. These alloys are of particular interest because Niobium is recognized as a β-phase stabilizer, implying a lower elastic modulus than α-type alloys, such as $cp-Ti$ grade 4, and $\alpha\ +\ \beta$-type alloys, such as $Ti-6Al-4V$. In addition to being formed exclusively by biocompatible elements [46], another motivation for developing these alloys is the possibility of substantially altering the microstructure of β-type alloys through heat treatment or cold work. The

binary systems Ti-Nb can be found relatively quickly in the literature, although there is a difference between the references due to the thermodynamic model used to calculate them. In Figure 3.2, it is possible to verify that Niobium is an element with a strong ability to stabilize the β structure of titanium and increase the alloy's melting temperature.

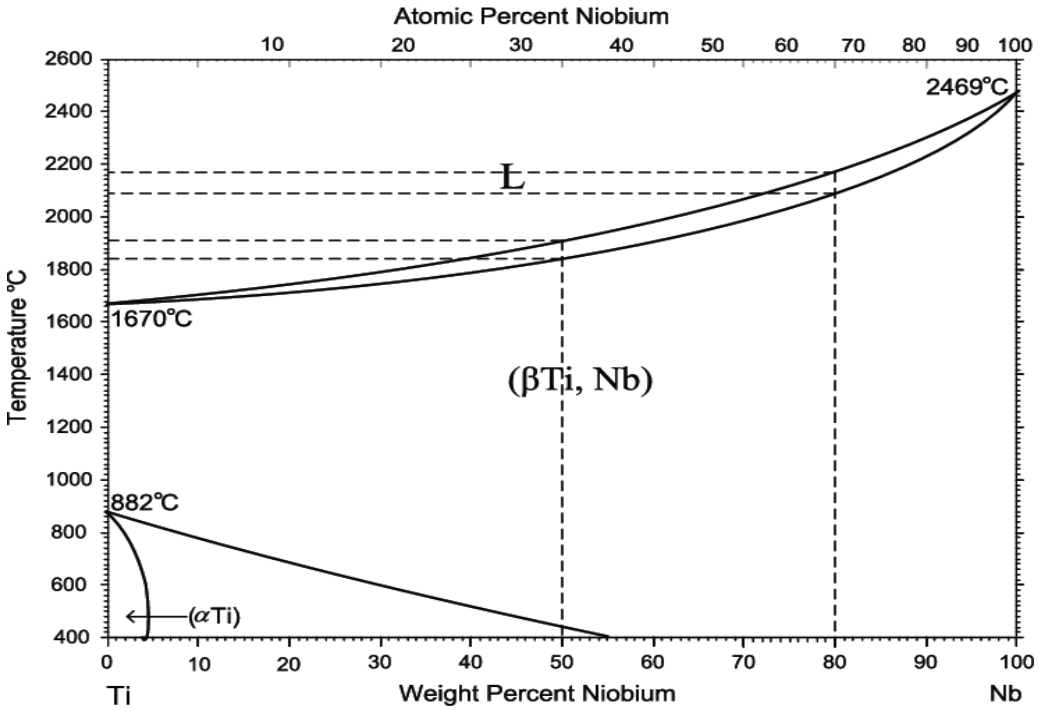

Figure 3.2 Phase diagram in the equilibrium of the $Nb - Ti$ binary system [47].

The phase equilibrium diagram of the $Ti - Nb$ system is of the isomorphic type, without invariant reactions or congruent transformations. Due to Niobium's much higher melting point than titanium, the alloy's melting temperature will become more significant as the niobium concentration increases. It has been observed that increasing the concentration of Niobium results in a decrease in the alloy's β-transit temperature, demonstrating its β-stabilizing properties. The cooling conditions offer structures closer to equilibrium than those obtained by oven cooling. Using this cooling in Ti-Nb alloys, for amounts of Niobium above 35% by weight, the microstructure is entirely constituted by the metastable β phase [47].

Titanium alloys with up to 15% Nb by weight and subjected to sudden cooling obtain an essentially martensitic structure of the acicular α' (hexagonal) type. Along with the range of values between 17.5% to 35% Nb, rapid cooling leads to the formation of α" (orthorhombic) martensite. In addition to the $\beta\ phase$, quenching of Ti alloys

containing Nb can form small amounts of ω phase when the Nb content is between 15% and 30% [48].

It is known that β titanium alloys, when cooled, can form α' (H.C.) and α" (orthorhombic) martensitic phases. Furthermore, it is possible through an athermal or even thermal transformation (by aging) that the β phase gives rise to the ω phase, usually responsible for an increase in the brittleness of titanium alloys [31]. These metastable phases are not shown in most equilibrium diagrams. However, understanding the ternary diagram for different temperature ranges helps to properly plan heat treatments to suppress or stimulate the appearance of these phases, depending on the desired application. The later section will explore the influence of heat treatment on the stability of these metastable phases.

These titanium alloys are good options for implant materials, but they can't stop bacterial colonization once contaminated. If contaminated materials are inserted during surgery or bacteria from the mouth fill an already placed dental implant, antibiotic treatments will be necessary; however, these therapies may not be effective against antibiotic-resistant bacterial strains. As a result, $Ti - Cux$ binary alloys, which copper is alloyed with titanium to generate an intrinsic antibacterial activity, have been a hot research topic [49]. The popularity of this metal alloy has sparked research into the $Ti - Cu$ alloy system's transformation kinetics, which has demonstrated how active transitions occur [50]. Other studies have looked at the optimization of $Ti - Cu$ alloys [51] and the biocorrosion of the materials [52]. However, doubts about the intermetallic compounds present, Ti_3Cu and/or Ti_2Cu, remain unanswered, with metastable Ti_3Cu not being reported in specific research [53].

Furthermore, reactive oxygen species have been hypothesized as a source of Cu ion impacts on antibacterial processes [54], although details concerning Cu ion toxic doses have remained unresolved. Finally, ternary titanium alloys [55] have been alloyed with Cu, α-eutectoid stabilizer, Cu has several exciting effects in ternary and higher-order alloys, but further study is required to comprehend them properly. Therefore, this thesis aims to add to the existing body of knowledge by investigating copper-containing titanium alloys.

Ho et al. [56] studied the mechanical properties of alloys containing molybdenum and showed that this binary system is promising. Chen et al. [57] analyzed these alloys' microstructure and mechanical properties, ranging from 5 to 20% molybdenum by

weight. The alloys were obtained by casting, and no mention was made of quenching or other heat treatment. The increase in molybdenum is directly associated with the β-phase fraction present; consequently, a decrease in the elastic modulus was observed, in addition to a considerable increase in ductility. However, a loss of compressive strength was observed.

3.3 APPLICATION OF Ti AND ITS ALLOYS IN MEDICINE

Ti and its alloy alloys are frequently used in biomedical devices and components due to their advantageous properties, such as good fatigue strength, biocompatibility, machinability; corrosion resistance, and a relatively low modulus; particularly as hard tissue substitutes and in cardiovascular applications and cardiac. However, not all clinical requirements can be met by titanium and its alloys [30].

Due to its resistance to corrosion in a physiological environment, high strength-to-weight ratio, low modulus of elasticity, and resilience to fatigue pure titanium, several of its alloys have been utilized extensively as "load-bearing" implants for biomedical purposes [58].

Figure 3.3 depicts a schematic representation of the human body's hard tissues. Accidents, aging, and other factors may all lead to the deterioration of hard tissues. Artificial replacements for injured hard tissue are often used in surgical procedures. The needs of various endoprosthesis materials vary depending on the area where the implants are put and the functionalities to be given [59].

The incompatibility of bone's Young's modulus (10–30 GPa) with metallic implants in orthopedic surgery is one of the critical issues with metallic implants ($110\ GPa\ for\ Ti\ and\ 105\ GPa\ for\ Nb$). Incompatibility causes the so-called "stress shielding" to be underloaded in the bone. Compared to complex biological tissues, Young's modulus of most metals is 10-20 times higher. Bone remodeling and stress shielding have been found in several studies to reduce healing and increase bone porosity.

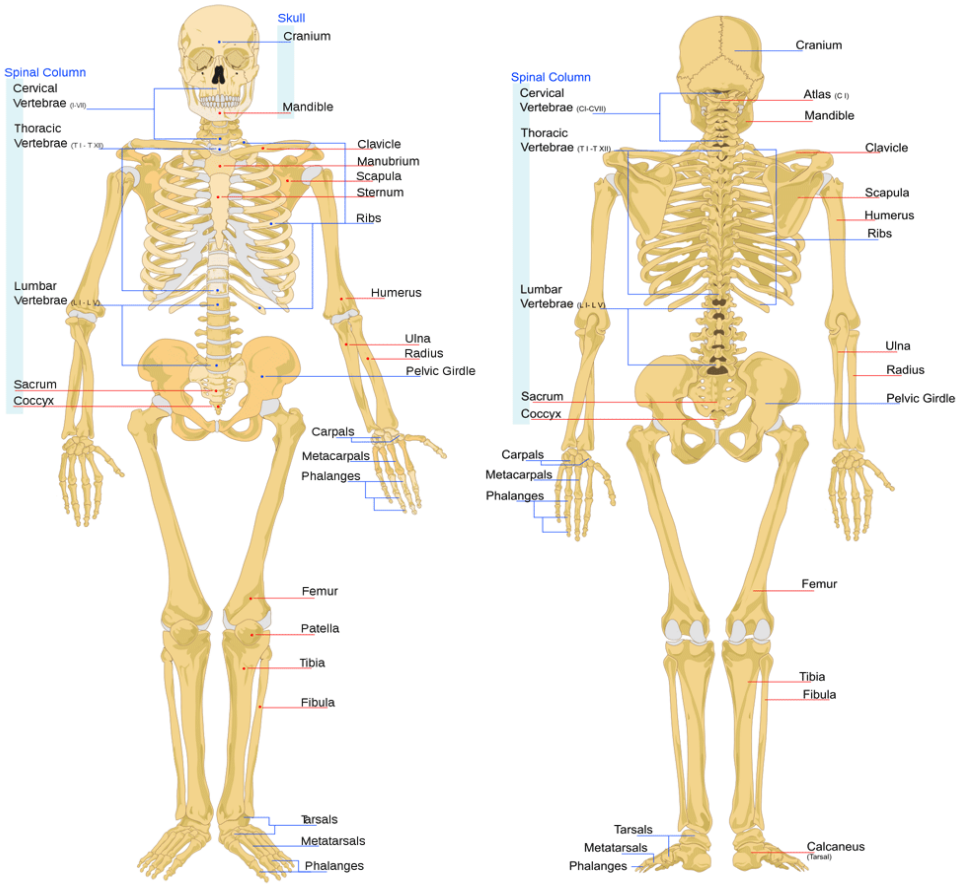

Figure 3.3 Human body hard tissue [59].

The presence of pores is one solution that may help ease the problem and lower Young's modulus of metallic materials. This will also help minimize damage to the tissues close to the implant, ultimately leading to a longer lifespan for the device [60]. Figure 3.4 shows three different-sized types of Ti powder grains.

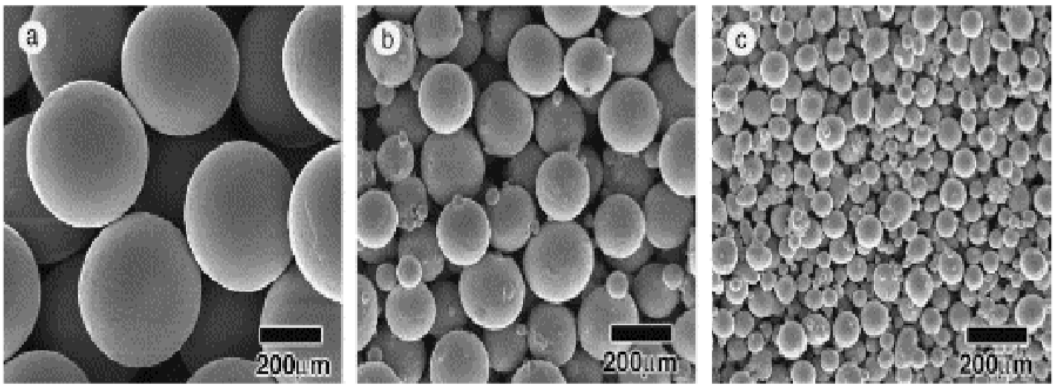

Figure 3.4 SEM of Ti powders with three different powder sizes [60].

Ti and its alloys are often utilized as hard tissue replacements for dental implants, artificial bones, and joints because they possess the ideal qualities described above, as seen in figure 3.6. As shown in Figure 3.5, artificial hip joints are one of the most popular uses for Ti and its alloys. These joints consist of a joint bearing (femoral head and cup) and a stem to connect the two components of the joint. While the trunk ensures that the femoral head is securely positioned concerning the other assembly components, the articulation bearings must be positioned to mimic the natural movement inside the hip joints. The intramedullary canal of the femur serves as a stable anchor for the hip stem, which is permanently attached to it. The femoral head's joint partner, the cup, is utilized to ream an attachment socket in the acetabulum. Additionally, titanium and titanium alloys are often utilized to replace knee joints, including femoral, tibial, and patella components [61].

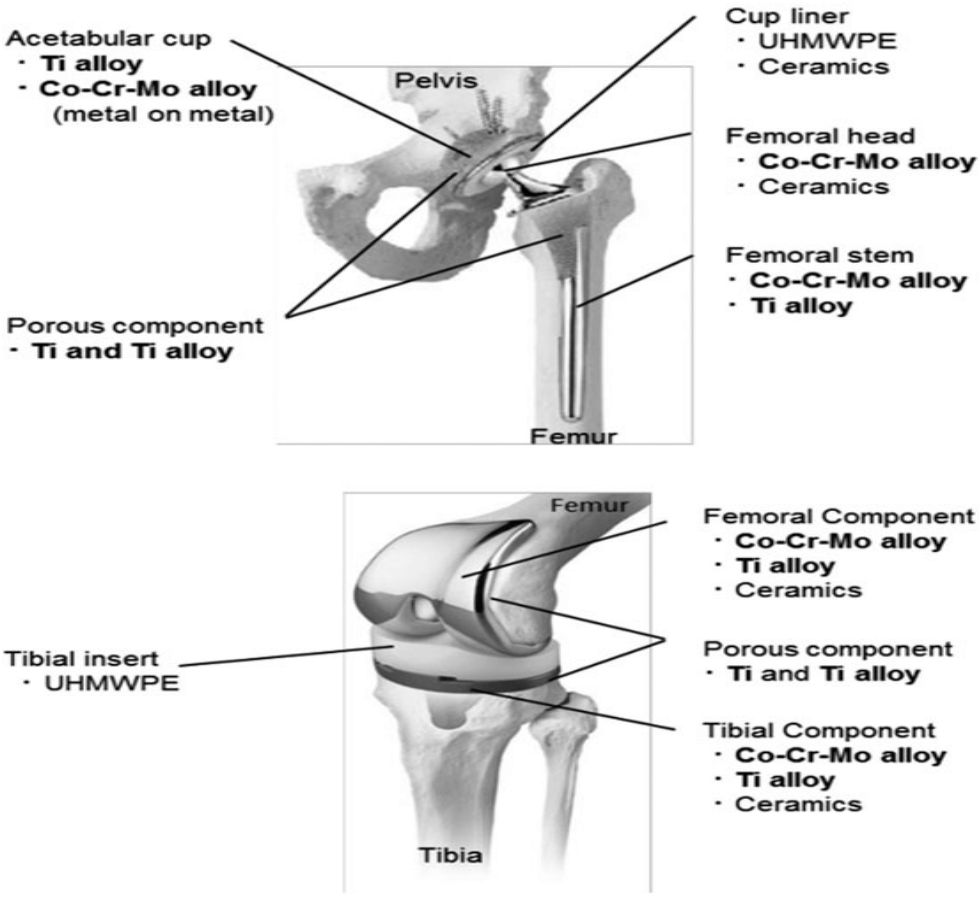

Figure 3.5 Schematic drawing of Ti-alloy in the artificial hip joint [61].

In addition, dental implants, categorized as subperiosteal, transosteal, and prosthetic based on their location and form, often use titanium and titanium alloys. Subperiosteal implants are made to fit snugly against the bone and sit just below the mucoperiosteum.

Posts or pillars implanted through the oral mucosa hold the prosthesis in place. Although transosteal implants are only suitable for the lower front jaw, osseointegrated implants may be implanted in the lower and upper jaws through a mucoperiosteal incision [62]. They are the most popular implants since they may be used to replace a single tooth, several teeth, or even a whole arch of teeth in instances of partial or complete tooth loss. Root-forming implants are the most popular kind of osseointegrated implant. Standard configurations, including the screw and cylinder shapes, are seen in Figures 3.6 and 3.7 [63].

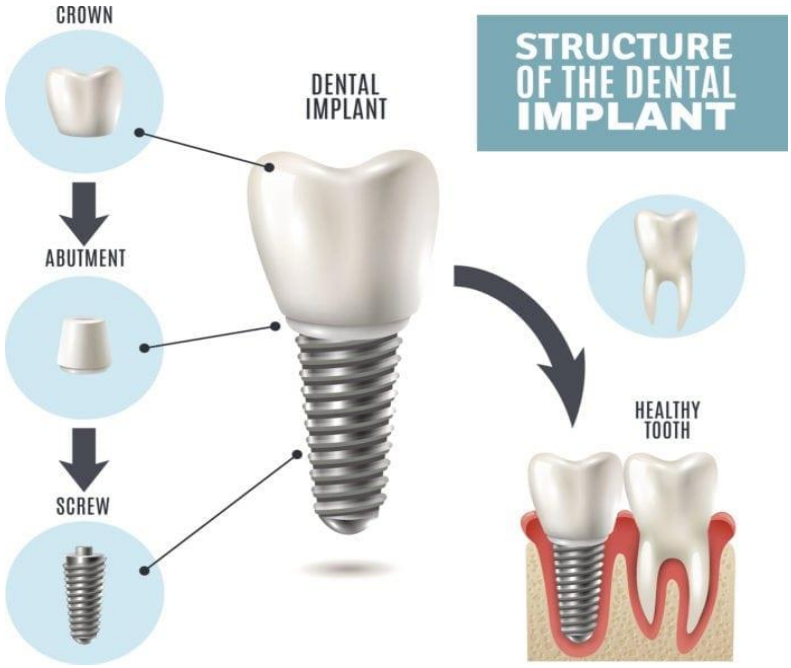

Figure 3.6 Schematic of the screw-shaped artificial tooth [63].

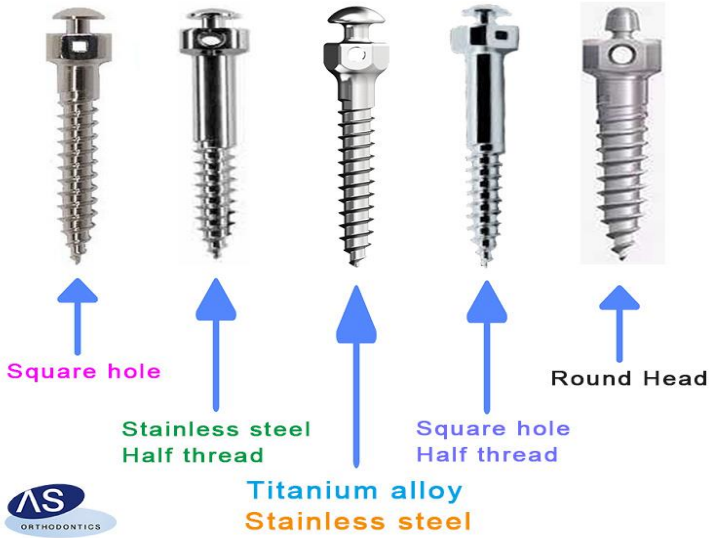

Figure 3.7 Types of Orthodontic micro screw dental [63].

The concept of osseointegration, which enables dental implants to bond with the bones after they have been put, is used in the placement of these dental implants. Surface modification methods such as plasma spraying, chemical etching, and blasting ammunition are often used to improve the osseointegration capabilities of Ti dental implants. Figure 3.8 depicts a metal plate for a fixed full denture, a partial denture, crowns, and bridges composed of Ti-15Zr-4Nb-4Ta alloys. Some other uses of titanium alloys may be found in oral prostheses. A whole denture metal plate, partial denture metal plate, partial denture, and partial denture metal plate radiography.

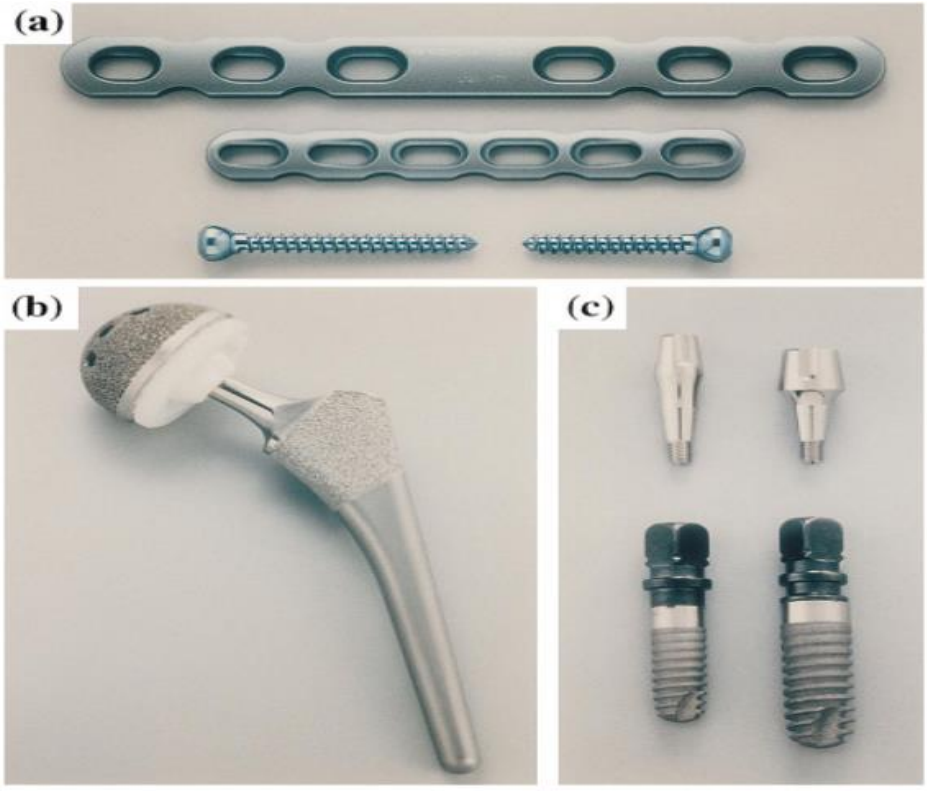

Figure 3.8 Implants: (a) cemented-type artificial hip joint (b) and artificial tooth root (c) $Ti-15Zr-4Nb-4Ta$ alloy dental posts [64].

Many types of valve prostheses have been used clinically. The typical design is shown in figure 3.9 [65]. Ti and its alloys are used in constructing the ring and holders, while pyrolytic carbon is used to make the disc. A sewing ring made of Teflon mesh cloth is wrapped around the ring, where the sutures that attach the prosthesis to the heart are put. Carbon coatings are often used to improve the compatibility of metals used in prosthetic valves with blood.

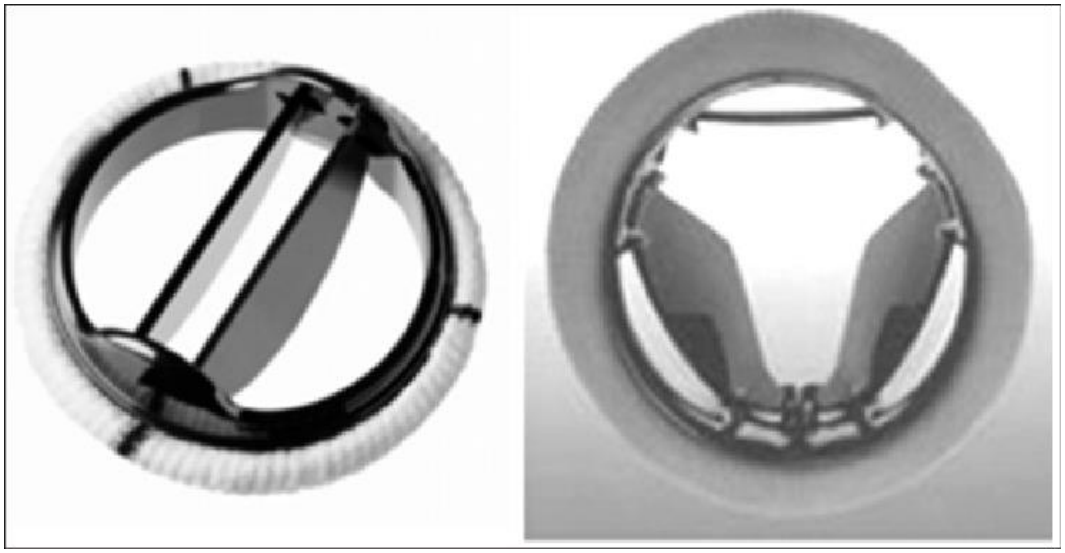

Figure 3.9 Heart valve [65].

Currently, stents like those shown in Figure 3.10 are often used to treat cardiovascular disorders. Narrow blood arteries are kept open via dilation. Balloon catheters or specialized delivery catheters are often used to transport stents to their intended locations. Nickel and titanium alloys exhibit unique shape memory characteristics and are the materials of choice for vascular prostheses [66].

Figure 3.10 Artificial vascular stents [66].

Ti and its alloys are often employed in osteosynthesis, which includes bone fracture repair, in addition to their application in joints, dental implants, and artificial bones. When a bone breaks, the affected limb can no longer be used. Osteosynthesis, the surgical repair of bone fractures using titanium alloys, allows for a speedy and comprehensive recovery [67].

Because of its unique qualities that suit the criteria of osteosynthesis applications, Ti and its alloys are appealing as an implant. Bone plates and screws used in osteosynthesis are examples of common implants. As shown in Figure 3.11, maxillofacial implants may be used for direct bone fixation with a single screw, often placed using "lag" screws that provide compression throughout the fracture gap, or they can be used to secure plates or other devices to the bones [68].

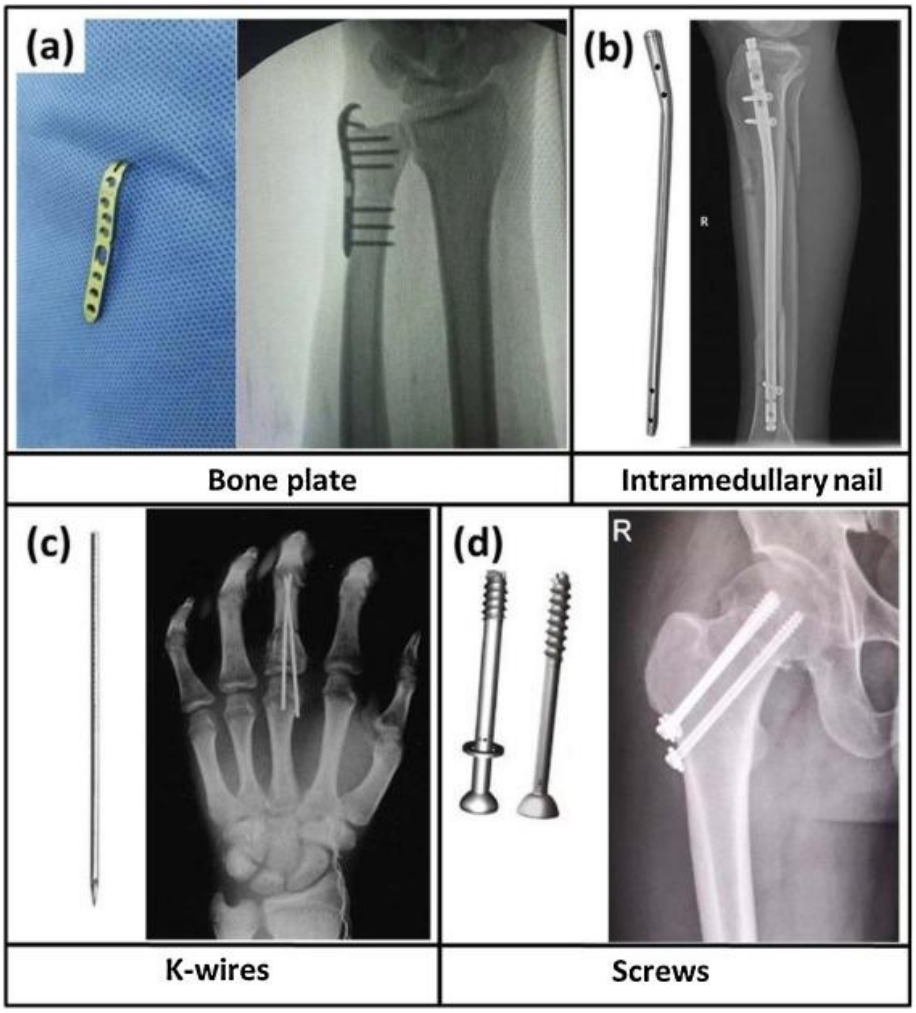

Figure 3.11 Bone plate and screw prostheses [68].

3.4 ELECTROCHEMICAL BEHAVIOUR OF TI AND ITS ALLOY

Corrosion may occur in any metal or alloy that comes into contact with human fluids because of how harsh the body's environment is. The surface of an implanted material undergoes a broad range of chemical changes. Passive coatings on the surface of most metallic materials used as implants keep corrosion rates low even though corrosion may inflict a wide variety of harm [69].

Although metals used in implants have good corrosion resistance, migration of metal ions to tissues or body fluids occurs. The corrosion resistance of the metal, the surrounding environment (chloride ion concentration, pH, etc.), mechanical factors (film adhesion, existing cracks, and surface abrasion), electrochemical effects (potential, galvanic effects, corrosion), and cell concentration close to the implant all influence the number of ions released [70].

Body fluids have a very complex composition, consisting of chloride, phosphate, sulfate, amino acids, and proteins ions, and this complexity associated with the presence of dissolved gases such as carbon dioxide, nitrogen, and oxygen makes body fluids suitable for the development of electrochemical processes [71].

Electrochemical techniques in media that simulate physiological fluids are widely used to evaluate the corrosion behaviour of metallic materials intended for biomedical applications [72].

Among the existing electrochemical techniques, we can mention [73]. Open circuit potential measurements – determine the corrosion potential in an electrolyte, and its value can be used to predict the long-term functionality of a metallic structure. A non-destructive test called linear polarization is used to identify a test electrode's steady state. The metal's corrosion rate is estimated using polarization resistance.

Anodic polarization is a test to evaluate the effectiveness of a passive coating in preventing corrosion and characterizing the corrosion behavior of the metal. The Tafel constants and the corrosion current Icorr are calculated using cathodic and anodic polarization, respectively. The primary cause of restrictions in the biocompatibility of materials is corrosion products, which may also cause unfavorable responses in tissues around the implant [73].

Titanium is corrosion resistant in all-natural environments, such as air (polluted or with ocean moisture), soil (mineral salt type environment), and most industrially contaminated water. For these reasons, between 20 and 30% of titanium consumption is concentrated in applications requiring corrosion resistance [70]. Titanium alloys are corrosion-resistant due to a film composed mainly of TiO_2 that covers the metallic substrate. This film is spontaneously formed on the surface of Ti alloys when exposed to the atmosphere [39].

Several studies are focused on the evaluation of corrosion resistance in titanium alloys. Cemasco [74] used electrochemical tests (polarization and impedance curves) to evaluate the influence of microstructure on the corrosion resistance of $Ti-35Nb$ alloy in $0.9\%\ NaCl$ medium at 25°C. It was observed that the studied alloys presented the same passivation current (ipp = 8.30 μA) and that the alloy submitted to oven cooling presented a more noble corrosion potential when compared to the alloy in the water cooling condition.

Martins et al. [75] $Ti-30Nb$ alloys were investigated in a $0.9\%\ NaCl$ $(0.15\ mol/L)$ solution at room temperature, and the addition of Zr (7.5 and 15% by weight) was shown to improve corrosion resistance.

Capela et al. [76] also evaluated the corrosion resistance of alloys of the $Ti-Mo$ system in $0.9\%\ NaCl$ medium and found that the increase in the molybdenum content in the alloys (up to 10% by weight) makes the material more resistant to corrosion. This observation was verified through the open circuit potential (ECA) results, which were shifted to more positive regions and increased Rp values (polarization resistance) as a function of the concentration of molybdenum in the alloys, as illustrated in Figure 3.1. These results indicate a lower tendency to oxidize the alloy with increasing molybdenum.

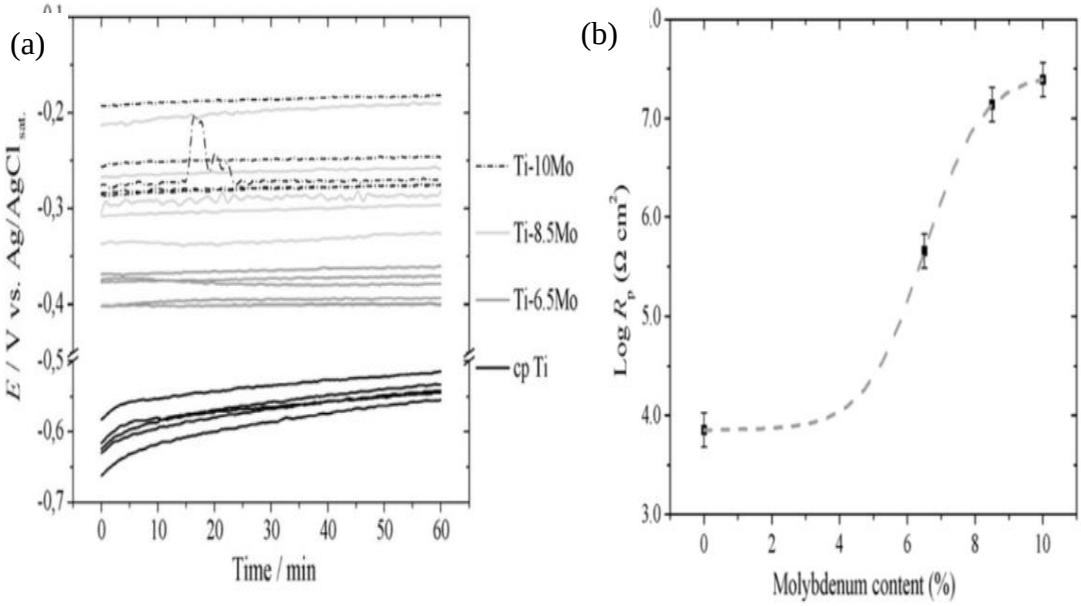

Figure 3.12 Curves of Open Circuit Potential (a) and polarization resistance (b) as a function of the concentration of molybdenum in the Ti alloy. Data were obtained in 0.9% NaCl medium [76].

Oliveira et al. [77] studied the electrochemical behavior $of\ Ti-Mo$ alloys (6–20 wt% Mo) in a solution that simulates body fluid. The values of the open circuit potentials indicated that the studied alloys undergo a spontaneous passivation process due to the formation of the oxide film on the metallic surface. It was also observed that alloys containing up to 15% Mo formed oxide films with better protective characteristics.

The results observed in the works described by Capela et al. [76] and Oliveira et al. [77] can be explained by the concentration of molybdenum in the alloys. According to the authors, adding molybdenum to the alloy significantly increases the grain size. When the amount of Mo in the alloy is low, the grains formed are smaller, thus increasing the relative grain boundary area, making the material more susceptible to corrosion. On the other hand, when the amount of Mo increases, the grain size also increases, thus reducing the surface area of grain boundaries, making the alloy less susceptible to corrosion.

Metikoš -Huković et al. [78] investigated the influence of Nb and V on the corrosion resistance of Ti- alloys used for implants in a physiological environment. The authors noted that the presence of these elements increases the corrosion resistance of the alloys, and the alloy of composition $Ti-6Al-16Nb$ exhibited a higher Rp than the alloy $Ti-6Al-4V$. This means that the oxide film formed for $Ti-6Al-16Nb$ is more adherent, compact, and resistant than the film formed for $Ti-6Al-4V$. It is important to emphasize that studies related to evaluating corrosion resistance in $Ti-Nb-Si$ alloys are scarce, making this work even more relevant from a scientific and technological point of view. Because of this perspective, studying the corrosion resistance of $Ti-Nb-Si$ alloys intended for orthopedic implants becomes necessary since the corrosive behavior can compromise the performance of these materials, altering their mechanical properties and biocompatibility and thereby reducing the lifespan of the prosthesis.

3.5 ANTIBACTERIAL STRATEGIES FOR IMPLANTS

Antibiotics have been the standard therapy for peri-implantitis since it was first discovered in clinical practice. Recently, antibiotic resistance has become a serious healthcare issue, making it impossible to continue prescribing ever-stronger medicines [79]. The development of innately antibacterial biomaterials is consequently a critical factor in preventing peri-implantitis. Essential oils have been utilized to treat bacterial

colonization and show antibacterial effectiveness in the food packaging sector [79] and in treating dental caries against Streptococcus mutans in various techniques that have been established to date. Other researchers have looked at polymers with nitric oxide, Pyridium content, and Pyridium-containing polymers that were more efficient than the antibiotic Amoxicillin in reducing bacteria. In addition, antibacterial effects have been achieved by varying the roughness of a material's surface. According to one study, Staphylococcus epidermidis germs are less likely to adhere to a rough surface [79].

Cao et al. [10] observed that the "spears" and "pockets" present in nanostructured surfaces reduced the amount of the same bacterium on the surface (Staphylococcus epidermidis). Silver (Ag) in magnetron-sputtered coatings has shown significant antibacterial capabilities, and thin films for antibacterial surfaces have also shown these qualities. However, problems with Ag segregation in thin films and early ion release into the environment remain unclear [10]. Silver alloys have also been developed as antibacterial substances. It has been found that when zinc (Zn) and copper (Cu) are added to a Si-O x thin film, copper (Cu) is more effective in reducing bacteria. Cu in Ti-Cu thin films likewise exhibited this potent antimicrobial capability; nevertheless, both materials exhibited osteoblastic toxicity after the first release of ions. While the Ag-Ti antibacterial action has been used for some time, it has been paired with photochemical processes to create reactive oxygen species (ROS), which has led to a UV-induced stress response in bacteria [10]. While these solutions have shown bactericidal effectiveness, there has yet to be a definitive material answer to the bacterial challenge.

As a result, efforts to alloy Copper to alloys in bulk materials have recently been explored and shown to be successful at a bacterial reduction, with the theory that liberated Copper ions aid in this antibacterial action. Copper ions have a partial action, according to further studies. Further research led to the concept that Cu ions participate in Fenton processes to produce reactive oxygen species (ROS), preventing bacteria from replicating 16SrRNA and resulting in death [11]. Aside from the effects of Copper ions, bacteria have been shown to die when they come into direct touch with a Cu-containing surface. Copper in titanium alloys has sparked renewed attention and has been recommended as a potential material for future implants. Given the promising aspects of alloying and the superiority of Copper over other elements in preventing bacterial growth, it is suggested that more research into the development of $Ti - XCu$

alloys would be beneficial and lead to a better understanding of this area, allowing for better future management of the bacterial burden associated with dental implants. This thesis aimed to investigate these materials' antibacterial impact when they contact bacteria by introducing innate antibacterial capabilities into titanium alloys with copper addition [79].

3.6 BIOCOMPATIBILITY

Metallic biomaterials are widely used in medicine and dentistry to replace different tissues. This market is constantly growing due to technological evolution and population aging and has aroused increasing academic and industrial interest. Due to their excellent mechanical properties and production flexibility, metals manufacture hip prostheses, coronary stents, dental implants, knee prostheses, bone plates and screws, spine prostheses, and skullcaps, among other applications [80]. The primary metals used as biomaterials are SS, Co, and Ti alloys. Among these, titanium has a prominent position due to its good mechanical properties, but mainly for its ability to resist corrosion when in contact with body fluids and for its biocompatibility characteristics superior to other metals, such as common allergic reactions and better biocompatibility between other metal alloys used [18].

Okazaki [64] demonstrates biocompatibility problems of these alloys due to the presence of these ions in Simulated Body Fluid (SBF) and animal tests. In extreme cases, stainless steel alloys such as 316L can cause significant adverse reactions to metalizing. Ni-Ti alloys, widely used by EMF, are associated with toxicity problems [81] and carcinogenesis [82]. Of the titanium alloys, $cpTi$ grade 4 and $Ti-6Al-4V$ alloys are the most used biomaterials. The $Ti-6Al-4V$ alloy was primarily developed for the aeronautical industry. Its application as a biomaterial has the disadvantage of having elements such as aluminum and vanadium, which are essential for the desired microstructure, but which, when undergoing the corrosion process when subjected to the body environment, release aluminum and vanadium ions that are associated with immune and adverse responses of the organism. local tissue [46]. In addition, the $Ti-6Al-4V$ alloy has a modulus of elasticity of $100-120\ GPa$, much higher than the modulus of elasticity of bone of 10-30 MPa, causing local bone resorption, a phenomenon known as Stress Shielding [83]. The $cp-Ti$ grade 4 has no toxic ions in the body and has good mechanical properties, and is considered the

current Gold Standard. This alloy responds well to surface treatments commonly used to increase biocompatibility. However, as in the $Ti-6Al-4V$ alloy, it has a high modulus of elasticity (>100MPa) when compared to bone [69]. One of the primary motivations for developing β-type titanium alloys is the expectation of developing an alloy with good mechanical properties, a modulus of elasticity closer to the bone, and the possibility of working with non-toxic β-stabilizing elements in the body. Figure 3.13 below shows the modulus of elasticity of various alloys applied as implants.

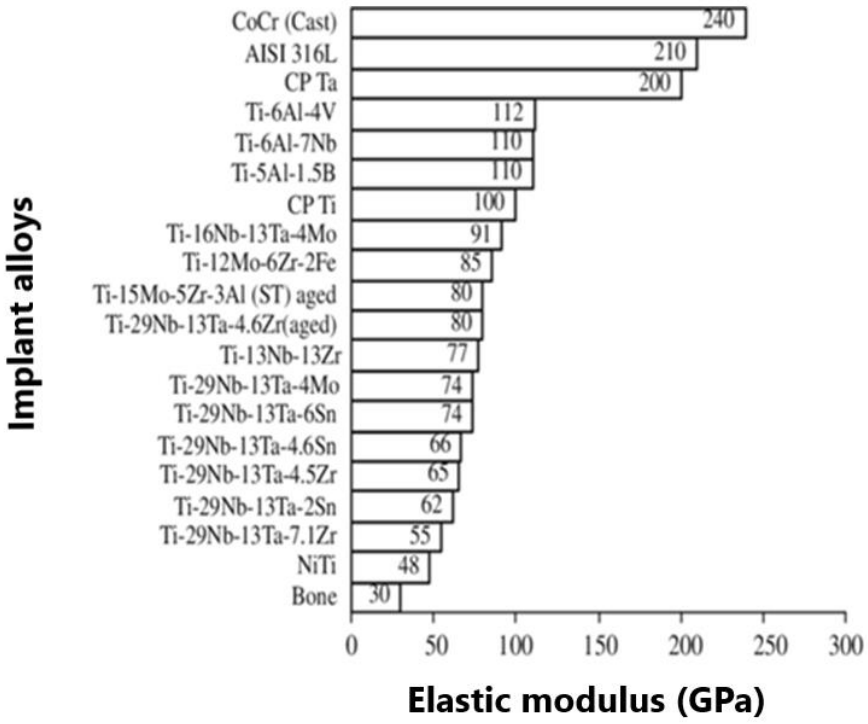

Figure 3.13 Elasticity modulus for various alloys in implants [69].

In order to confirm the benefit of using alloys with a low modulus of elasticity, several studies have been developed over the last few years, establishing a consensus in the literature on the subject. As an example, we can mention [84]. The fracture was induced in the tibia of rabbits, and alloys of $Ti-29Nb-13Ta-4.6Zr, Ti-6Al-4V\ ELI, or\ SUS\ 316L$ were used to fix the fracture. X-rays analyzed bone turnover, recovery, and atrophy from two to 24 weeks.

Niinomi [63]compared the modulus of elasticity of $\beta\ titanium\ alloys\ (Ti-13Nb-13Zr\ and\ Ti-25Nb-13Ta-4.6Zr)\ with\ Ti-6Al-4V\ ELI$. The $\beta-type$ alloys were divided into two groups, one that underwent hard work to improve the mechanical properties by work hardening and another that, after the cold work,

underwent an aging heat treatment at temperatures from 300 to 400 ºC for 259 ks. As expected, heat treatment substantially alters the microstructure of β-type alloys. It was found that the heat treatment for the two β alloys increased the modulus of elasticity but was still below the $Ti-6Al-4V$. As mentioned in the previous section, this change is due to the precipitation of the α and ω phases after aging.

The cytotoxicity of $Ti-25Nb-13Ta-4.6Zr$ alloy was tested and compared with that of cpTi grade 4 and $Ti-6Al-4V$ with L929 cell counts in filtered and unfiltered solutions at 7 and 24 days. The results indicate that this β-type alloy has biocompatibility similar to $cpTi$ and superior to $Ti-6Al-4V$. Therefore, it is very promising for use as a biomaterial and reinforces the importance of low elastic modulus alloys, especially the β type [63].

Despite the $Ti-6Al-4V$ alloy having the lowest contact angle in the wettability test performed, its performance in cell adhesion was lower than the $Ti-35Nb-xZr$ alloys; this result reinforces that in addition to wettability, the chemical composition of the alloy is of high relevance in biocompatibility, being one of the main reasons for the search for new Ti alloys for biomedical applications [85].

3.7 Cu IONS IN MACROPHAGE INFLAMMATION

Cells and bacteria both make use of copper in their internal workings. In high quantities, the element functions in various enzymes for both, but it also has a harmful effect. Wilson's disease and Menke's disease are caused by excess or lack of Cu in humans. Most bacteria do not contain Cu ions inside their cytoplasm; instead, they are located only in the periplasm and plasma membranes of the cell. Furthermore, bacteria have a limited number of Cu-proproteins [79].

Instead, bacteria contain several Cu regulators, including CopZ and CopA A copper (Cu) transporter called CTR1 exists only in cells and is critical to embryonic development. To lessen the bacterial load, this transporter collaborates with ATP7A to move Cu from the cell to invading bacteria, including Salmonella enterica and Mycobacterium tuberculosis (T.B.) figure 3.14. Therefore, Cu is well-accepted as a pro-inflammatory agent that may benefit humans [79]. Mycobacterium tuberculosis (T.B.) has been demonstrated to have defenses such as the mycobacterial copper transport (mctB) B protein that continually pumps Cu out of the bacteria even though cells need Cu to eradicate germs and bacteria are sensitive to Cu. The virulence and

resistance of T.B. have been attributed to this protein. As a result, Cu is involved in several complicated interactions between bacteria and cells.

These interactions may also deter bacterial infection by using Cu ions. Studies on Cu ion dosage were conducted to determine Cu doses that promote cell viability while decreasing bacteria [79].

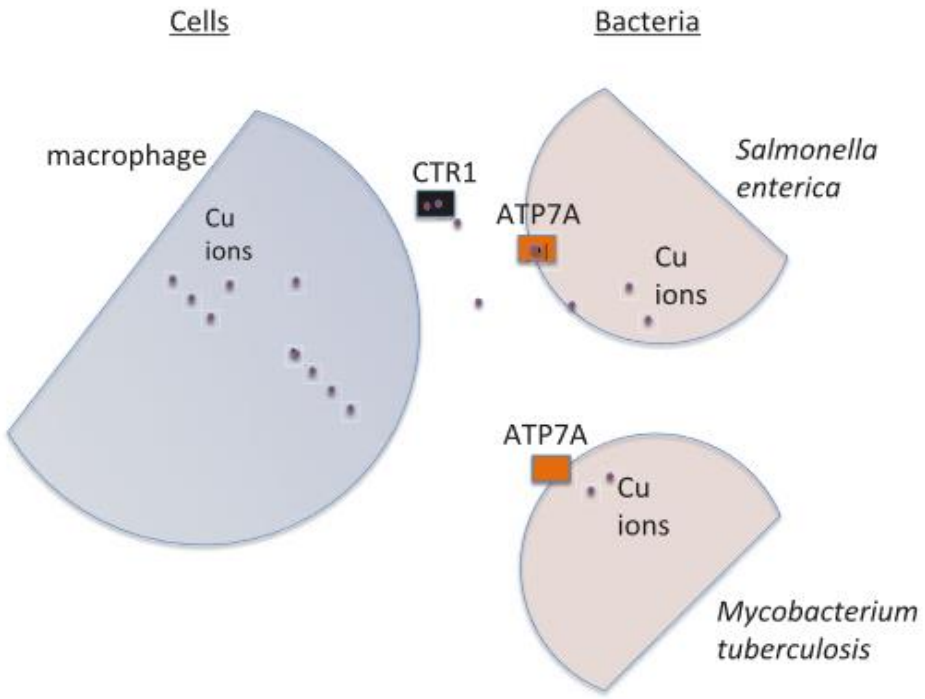

Figure 3.14 In vivo Cu ion transport via CTR1 and ATP7A [35].

3.8 PRODUCTION OF TITANIUM ALLOYS BY P/M METHOD

Powder metallurgy (P/M) is a technique for transforming metallic powders through compaction and consolidation of the part by controlled heating. It has well-defined stages: powder production, mixing/homogenization, compaction, and sintering. The P/M offers a viable tool for producing complex components, producing parts with complex geometry and dimensional tolerances close to the final sketch. This technology uses approximately 90% of the raw material, possibly avoiding or limiting the machining process, producing components with a good surface finish. Another essential feature is the ability to precisely adjust the chemical composition, densification, and microstructural homogeneity. These factors contribute to a reduction in production costs compared to conventional processing. Mainly this applies to relatively expensive materials such as titanium alloys [86].

The high cost of extracting and manufacturing titanium makes it difficult to use it widely for conventional engineering, aerospace, and medical implant applications. This generated the need for inexpensive alternatives for producing titanium, with P/M being presented as the most economical. Pre-alloyed (PA) and Blended elemental (BE) are two common approaches to obtaining titanium alloys.PA uses pre-alloyed powders that can be obtained, for example, by atomization, with subsequent compaction using hot isostatic pressing. However, it is costly despite producing components with excellent mechanical properties. The BE technique involves mixing elementary powders without the high costs referred to in the first process. The later steps are isostatic cold pressing, followed by sintering or uniaxial hot pressing. The elemental mixture is characterized by the low density of the products, about 95% of the theoretical density, while PA produces completely dense components.

However, with advances in the BE technique, it is now possible to produce products with 99% of the theoretical density using hydrogenated powders. Hydrogenation is the saturation of hydrogen atoms in the material's crystal lattice through controlled heating. Hydride particulates are obtained by comminution (generating a wide particulate distribution) or the milling process (obtaining more significant control of particulate distribution). The removal of hydrogen from the material consists of the dehydrogenation step during heating under a vacuum. The chemical reaction of this process can be written as $M + H2 \leftarrow \rightarrow MH2$, where (M = metal), the two arrows symbolize the reversible reaction. The hydrogen gas pressure controls the reaction's direction; if the pressure is higher than the equilibrium pressure, the reaction moves to the right and produces a metal hydride. The metal hydride dissociates into metal and hydrogen gas if the pressure is lower than the equilibrium pressure [86].

The subsequent steps in the process of obtaining powders are compaction and sintering. The first consists of the conformation of the powders, and the second is the final consolidation of the part. Sintering is the transport of matter in a mass of powders or a porous, thermally activated compact. It reduces the free specific surface by the growth of the contacts between the particles, the volume reduction, and the geometric alteration of the pores. There are two sintered product lines of interest to the industry. One focuses on densification and increasing strength without necessarily introducing dimensional changes. Another line is the production of elements that present a minimized densification; that is, they present a controlled porosity. Some parameters

are necessary to satisfy the quality of the sintering process, such as the controlled conditions of heating and cooling speed, ambient atmosphere, temperature, and time [87].

3.9 SINTERING PROCESS

Sintering is a physical process initiated by heat that enables a group of particles of a particular material to develop mechanical strength when they are first in contact with one another. This process is termed "sintering." The reduction in free energy associated with the surface of the set of particles, which may be accomplished by lowering the overall surface area of the system, is its primary driving factor [88]. In many cases, this results in a stiff and entirely or partly dense body due to eliminating the space between the particles [89]. The structural integrity of a part obtained by powder metallurgy is the result of sintering, where by heating at temperatures below the melting point, the particles are coherently joined together in a solid mass. Pores are eliminated while the particles unite during sintering at high temperatures; this temperature corresponds typically to 2/3 of the material's melting temperature [86]. Sintering is divided into three distinct stages.

Sintering is a solid-state diffusion process, where atomic movements and, consequently, diffusion occurs more rapidly with increasing temperature [90]. There is the possibility of performing sintering with a phase in the liquid state; this favors the bonding of metallic particles to each other and reduces the material's porosity [91]. The sintering process is related to the decrease in the surface energy of the particle, so a high initial area promotes faster sintering [90]. Pores can be interpreted as significant accumulations of vacancies; thus, the understanding of sintering is elucidated by its movement and, consequently, by diffusion. Four mechanisms of atomic movement occur in sintering: surface diffusion, diffusion along the volume, along the grain boundary, and by evaporation-condensation, as seen in figure 3.15 [92].

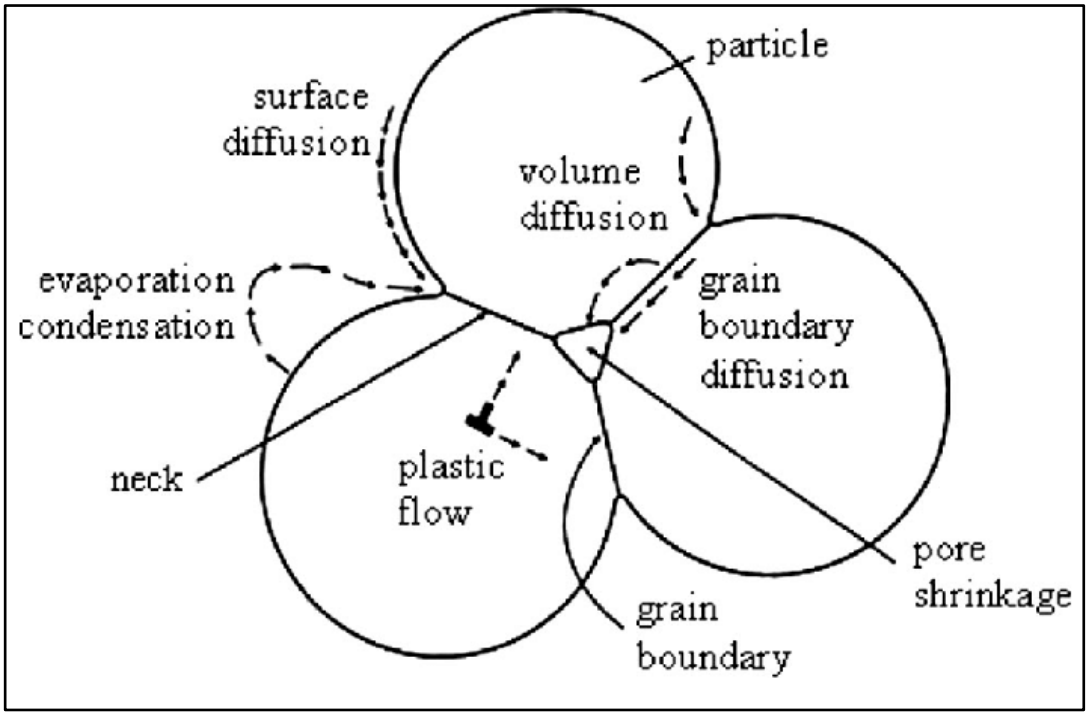

Figure 3.15. Mechanism of mass transformation during sintering [92].

Several theories try to explain sintering. The presence of the following stages can summarize these theories

a) Initial bonding between the particles and the formation of a neck occurs when the material is heated, leading to the formation of grain boundaries due to diffusion, occurring when there is intimate contact between adjacent particles .This initial step does not cause any dimensional change in the part but gives it great cohesion.

b) Neck growth: corresponds to a greater degree of bonding within the mass under sintering. At this stage, there is no decrease in the number of pores (contraction of the material), although this growth requires transporting material from the interior of the sintered mass.

c) Closing of the channels that make up the pores: a step that results in a considerable decrease in porosity. The cause of this closure is the growth of the neck and the contraction of pores.

d) Rounding of the pores: This step can be considered a natural consequence of neck growth. This step is promoted at high temperatures, and given enough time; it can make the pores perfectly spherical.

e) Pore shrinkage or densification: this is often considered the most critical step in sintering. The densification of the sintered mass only observes this step. This

densification can lead to both contraction and expansion phenomena. The contraction implies mass movement toward the pores.

f) Pore growth: corresponds to the tendency of tiny pores to migrate to larger porosities, causing them to increase in volume. The amount of pores decreases, but their volume remains unchanged. Other phenomena can occur in the mass under sintering and are also related to the decrease in the system's total energy. Grain growth is a dense and hardened material that tends to undergo three distinct structural changes when heated: recovery, recrystallization, and grain growth. Recovery corresponds to relieving material stresses without any noticeable structural changes. Recrystallization corresponds to the formation of new grains from an original hardened structure.

Both are related to the system's free energy reduction, resulting from the rearrangement or removal of crystalline defects such as dislocations. Grain growth in sintering will depend on controlling porosity and impurities (lubricants sometimes interfere with the process) in compacted samples. − Homogenization or alloying: sintering promotes solid-state diffusion of solute atoms in the solvent matrix and diffusion of solvent atoms into solute-rich particles. The kinetics of homogenization is complex, and mixing and mechanical work also influence the process. Inadequate mixtures can increase the interdiffusion distance and require a more extended homogenization treatment. − Phase transformation: according to the local composition of the site side, the temperature, and the pressure it presents, new phases can form [93].

PART 4

METHODOLOGY AND EXPERIMENT

4.1 INTRODUCTION

This section describes the procedures followed throughout the experiments, from collecting samples to analyzing them. The description of the devices used to conduct these tests in terms of the type and hand-manufactured and pre-addressed to these points need to be recognized throughout the technological process steps used in the current research to form a complete idea of the functioning of the production of samples and tests used in the recent study.

4.2. PROGRAM OF THE PRESENT STUDY

Samples coded in Table 4.1 were prepared in the present work, where the matrix alloy is based on ASTM F 2066-08 [94]. Figure 4.1 summarizes the overall program used in the present work.

Table 4.1 Prepared samples in the present study.

Sample No.	**The weight percentage of the element (wt.%)**		
	Ti	Nb	Cu
1	82	18	0
2	77	18	5
3	75	18	7
4	73	18	9

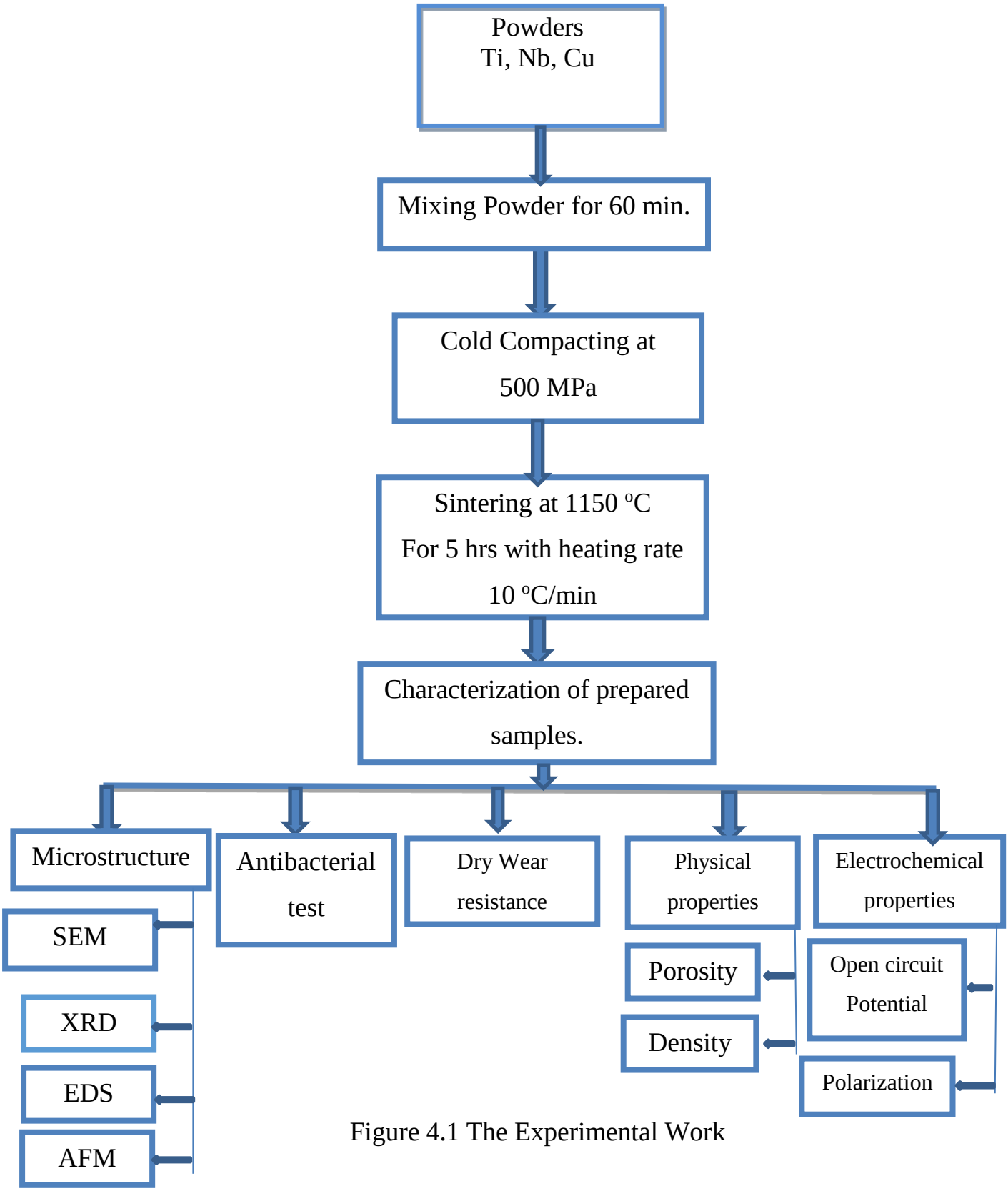

Figure 4.1 The Experimental Work

4.3. MATERIAL

To produce the Ti-18Nb-xCu alloys, a blended basic PM technique was used. To learn how much of an impact Cu addition would have on the characteristics of Ti-Nb alloy, four different weight percent (wt%) of copper were added to the mix: 0, 5, 7, and 9 wt%. Since the base alloy of Ti-18Nb was maintained, the rising copper content was countered by a falling Ti content. In Figure 4.2, the elemental powders of Cu (>99.5% purity sponge powder), Nb (99.8% purity), and Ti (99% purity).

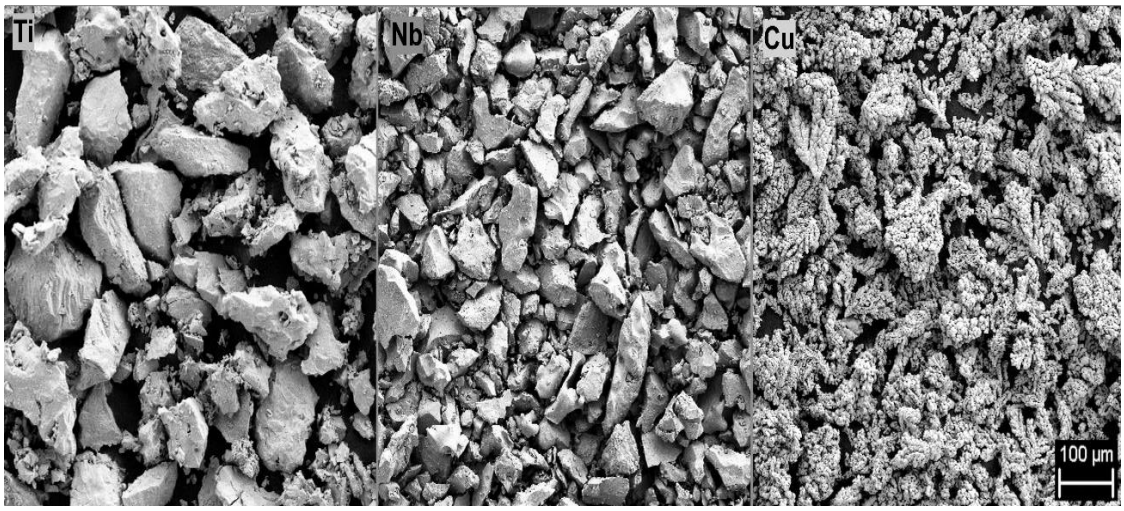

Figure 4.2. The general view of the elemental powders.

4.4 PREPARATION METHOD

For this experiment, dry ingredient powders were weighed and blended in a three-dimensional shaker mixer (Turbula) (60 min). The powder combination was uniaxially pressed at room temperature in a cylinder-shaped steel mold (13 mm in diameter) without applying lubricant or binder. It was determined that 500 MPa was the optimal compression pressure after testing 450, 500, and 600 MPa; thus, that pressure was applied to all samples (see Figure 4.3). Green samples were sintered for 5 hours at 1150 ° C in a Protherm PZF cylindrical tube furnace Figure 4.4 with an Ar gas atmosphere and a heating rate of 10 °C per minute.

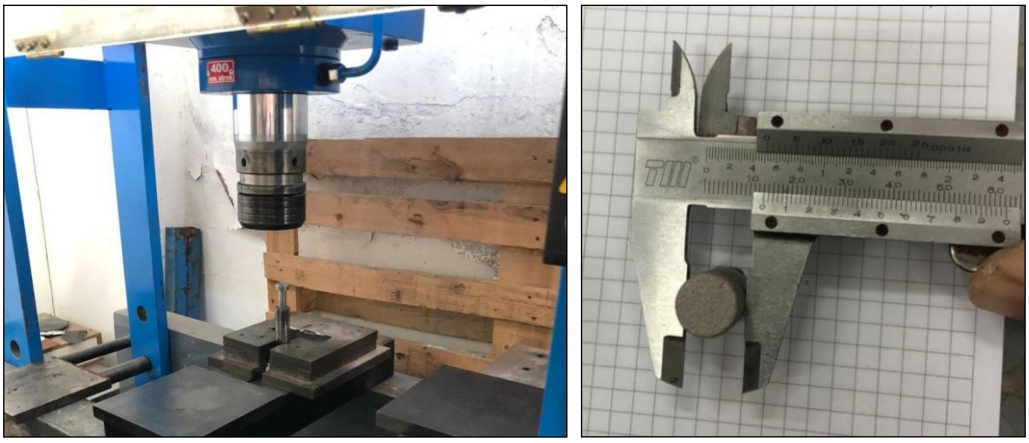

Figure 4.3. The pressing, mold, and diameter of the sample.

Figure 4.4. The tube furnace was used in this work.

To carry out the microstructural investigation, the cut samples were subjected, step by step, from grinding on SiC paper (240-1200 p) to polishing on 6µm diamond to etching with 5% Nital.

4.5 MICROSTRUCTURE CHARACTERIZATION

4.5.1. X-ray Diffraction (XRD)

X-ray diffraction analysis was used to examine sintered samples that measured 13 mm in diameter and 3 mm in height. The circumstances for the measurement are as follows: the target is copper, the wavelength is 1.54060 Å, the voltage is 30 KV with current is fifteen milliamperes, the scanning speed is 2 degrees per minute, and the scanning range is ten degrees to ninety degrees. X-ray diffraction was used to ascertain the matrix alloy phases and the reinforced particles, after which a comparison was made with the various standard charts.

4.5.2. Scanning Electron Microscope (SEM)

After the sintering process, the microstructures of the used specimens were taken using Scan Electron Microscope.

SEM test was used to obtain a chemical composition and its topography. The specimen is imaged through a high-pack of electrons; this test was done at the University of Karabuk –Turkey - using SEM type (Carl Zeiss ultra plus gemini FESEM), as shown in Figure 4.5.

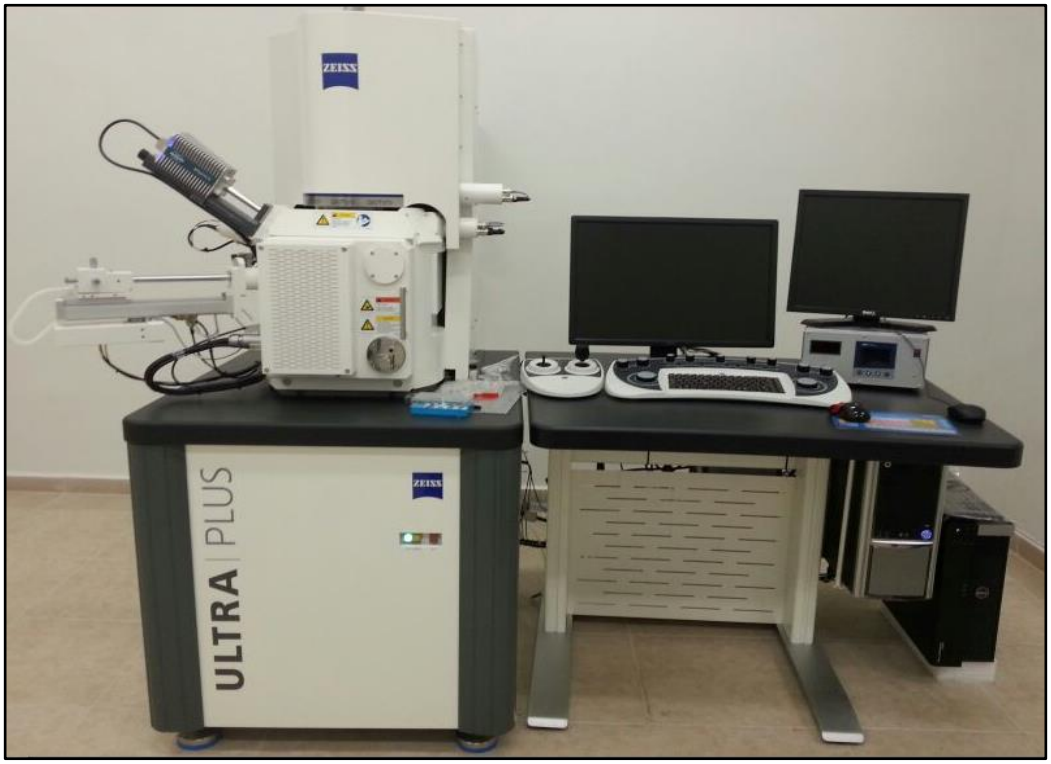

Figure 4.5 Scanning Electron Microscopy.

4.5.3 Energy Dispersive Spectroscopy

Energy-dispersive spectroscopy, often known as EDS, was used for chemical and elemental analysis of the materials. The EDS device was integrated with the SEM, and the examination was carried out in the manner shown in figure 4.5

4.6. PHYSICAL AND MECHANICAL TESTS

Following ASTM B327, porosity may be determined for the samples that have been sintered [39].

1- A vacuum drying furnace was used to dry the specimen at 100 ℃ for 5 hours while maintaining a vacuum (10^{-4}), and then it was cooled to room temperature. Mass A is used to represent the dry specimen's weight.

2-At room temperature, the specimen is placed in the oil for 30 minutes, where the pressure on the submerged specimen is reduced by using a suitable vacuum pump.

3-Mass B is the weight in the air after the oil immersion process.

4-Mass F is the specimen weight submerged in water.

5-Finally, through the following equation, it can calculate the porosity as the following equation:

$$p = \left[\frac{B-A}{(B-F)*D^{O}} * 100\right] * D_{W} \text{……..(4.1)}$$

$$\rho = \left[\frac{A}{B-D}\right] * D_{W} \text{ …….. (4.2)}$$

Where:

D_W – The density of water = 0.9956 g/cm^3.

D^O- The density of oil= 0.634 g/cm^3**.**

4.7 ATOMIC FORCE MICROSCOPY

To examine the surface's topography and determine its roughness, atomic force microscopy was carried out using a scanning microscope (NaioAFM 2022 Nanosurf Switzerland). A needle measuring in the micron range is moved over the surface scanned by the instrument. This needle is perpendicular to the holder and held in a horizontal holder. The laser beam is directed onto the holder, which rises and falls with the height and fall of the needle, and therefore with varying surface topography from high to low, and the receiver records the reflection of the laser beam on the holder.

Consequently, the scanned surface's topography may be determined and mapped based on how the laser beam's reflection moves.

4.8 DRY SLIDING WEAR TEST

The pin on the disc wear apparatus was used to conduct the wear test in the dry sliding environment following the standard ASTM G99-95. A schematic representation of the equipment may be seen in Figure 4.6. After each run, the specimen and the counter disc were cleaned with acetone and cotton to remove any material that would otherwise stick to them and cause problems. This was done in order to remove any residue left behind from previous runs. Before and after weight was measured using an electronic microbalance accurate to ±0.01 mg. The sliding wear test was conducted for varied applied loads $(5, 10, and\ 15\ N)$ throughout a continuous period (10 minutes), in addition to the other circumstances specified in Table 4.1. The following equation calculated the sliding wear rate (W.R) in (g/cm):

$$W.R = \frac{\Delta W}{S.D} \qquad (4.3)$$

where: ΔW is the change in weight before and after the test as $(W_2 - W_1)$ and S.D is a sliding distance (cm).

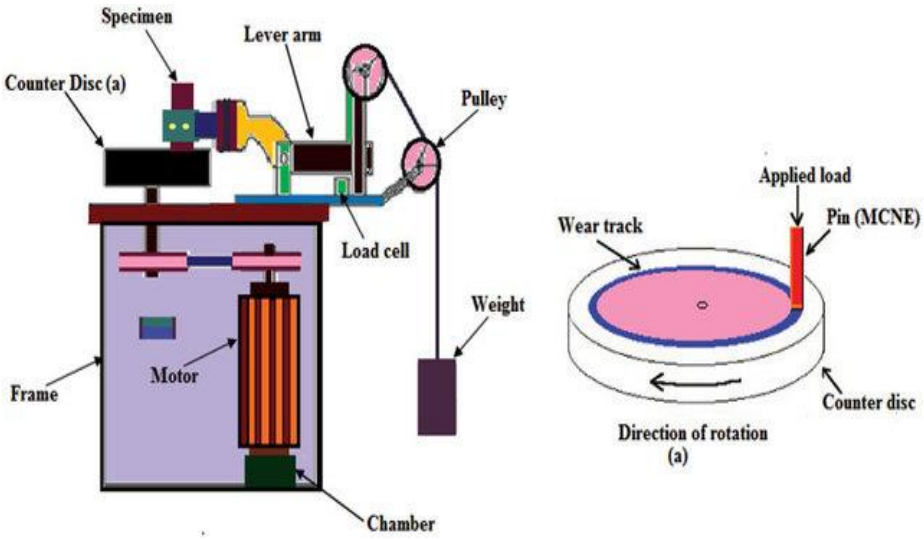

Figure 4.6. Schematic illustration of Pin on disc wear tester [95].

Table 4.1. Parameter of wear rate test.

parameter	Description
Still environment	Temperature $(27-29°C)$ and Humidity $(60-70\%)$
Specimen	Cylindrical Pin $\phi \approx 13 \times 25\ mm$
Counter disk	Steel with hardness $(358\ HV)$
Sliding distance	$6.5\ cm$
Applied load	$5, 10, and\ 15\ N$
Sliding speed	$1.887\ m/sec.$

4.9. CORROSION TESTS

The behavior of Ti and its alloys as implants in the human body has to be studied; thus, the corrosion test is used for pre-prepared samples in Ringer's solution with a Ph of 7.4 at 37 minus 1 ℃. Table 4.2 contains an illustration of the chemical compositions of the solution [96].

4.9.1. Open Circuit Potential

Calculate the Open circuit potential (OCP) for the pre-prepared specimens in Ringer's solution. Using Standard Calomel Electrode (SCE) to measure the working electrode potential, a voltmeter was connected between the working electrode and the reference electrode. For each specimen from (0 up to 60 min), open circuit potential measurements were performed. The first record was taken immediately after immersion; the voltage was monitored for the entire test period at 5min.

4.9.2. Potentiodynamic Polarization

An electrochemical test is often utilized to monitor the anodic and cathodic processes of corrosion (i.e., monitoring the corrosion reactions on a specimen of desired metal). The electrochemical CS 310 CorrTest workstation was used to conduct polarization experiments in Figure 4.7. All tests were conducted in a 1 L volume of Ringer's solution, to which a small amount of sodium bicarbonate ($NaHCO_3$) was added to bring the pH to 7.4.

The working electrode $(Ti-alloys)$, the auxiliary electrode $(Pt.electrode)$, and the saturated calomel electrode SEC reference electrode were all housed in a typical electrochemical cell with open necks. Tests were conducted on the corrosion resistance

of the samples in Ringer's solution at 371°C. To calculate the corrosion rate, one must use the following formula. [39].

$$Corrosion\ rate = \frac{0.13\ Icorr(Ew)}{\rho} \quad \ldots\ldots(4.4)$$

$$\mathrm{Ew} = \sum \frac{\text{Atomic weight}}{\mathrm{n_i} * \mathrm{wt_i}} \quad \ldots\ldots\ldots\ldots(4.5)$$

Where:

$E.W = equivalent\ weight\ (g/eq.)$

$\rho = density\ (g/cm^3)$

$0.13 = metric\ and\ time\ conversion\ factor$

$Icorr = corrosion\ current\ density\ (\mu A/cm^2)$.

$mpy = Corrosion\ rate\ (mils\ per\ year)$

$ni = valance\ electron$

$wti = weight\ present$

Table 4.2 Chemical Composition of Ringer's solution [96].

No.	**Components**	**Saliva Solution(g/l)**
1	KCl	8.6
2	$NaCl$	0.30
3	$CaCl2$	0.33

Figure 4.7. Potentiostat device.

4.10. ANTIBACTERIAL TEST

The agar well diffusion technique examined the materials' antibacterial effectiveness. Bacteria such as "Escherichia coli" and "Staphylococcus aureus" (both of which are gram-positive) were employed. After isolating the bacteria, we suspended them in a buffered saline solution and diluted them to 105 CFUs per mL in Muller Hinton agar. The agar was then drilled with a sterile cork borer to create wells of 5 mL capacity, and 20 L of dimethyl sulfoxide was added to each. The antibacterial effect was quantified by measuring the inhibition zone's size in millimeters (mm). We tested the antibacterial properties of Ti-18Nb-xCu alloys using the agar diffusion technique using the following experimental procedures:

1. $Escherichia\ coli$ Bacterial suspensions were obtained from cultures in nutritious broth for 24 hours, adjusted to 0.5 McFarland standard turbidity (1.5 108 CFU/mL), and diluted (1:10) to the appropriate bacterial density (1.5 105 CFU/mL).
2. c The bacterial suspensions (1.5 10 5 CFU/mL) were diluted to 0.1 mL and then plated on Mueller-Hinton agar.
3. Bacterial suspensions (100 µL) were spread on the surface of a 12cm Petri plate with Muller-Hinton agar with four alloys to evaluate antimicrobial activity and then placed on the surface of the agar and set for 5 minutes; then, the substrate of different concentrations of the tested method.
4. After incubating the plates at 37 °C for 18 hours, the micrometer was used to measure the size of the inhibition zone surrounding the discs. The antibacterial impact has been seen in the inhibition zone, with larger diameters indicating better antimicrobial activity of nanoparticles.

PART 5

RESULTS AND DISCUSSION

5.1 INTRODUCTION

In this part, the characterization of prepared alloys (Ti-18Nb-xCu) will be viewed by XRD, SEM/EDS analysis, and the exam of surface morphology will be scanned by AFM analysis. Dry wear behavior and corrosion resistance of experimental specimens were also measured to show the suitability of these alloys for biomedical applications.

5.2. CHARACTERIZATION OF ALLOYS

5.2.1. Porosity and Density

The chemical compositions of the prepared alloys with their measured average densities and calculated porosities are given in Table 5.1. The porosity of around 18% indicates that the alloy density can be increased. A similar effect (i.e., increasing density) can be observed by adding Zr element in ($Ti-13Nb-13Zr$) alloy to get 98.6% after sintering at 1250˚C for 4 hours and 360 MPa compression pressure [1]. The addition of Sn to the $Ti-16Nb$ alloy enhanced the density during sintering at lower temperatures, and this tendency continued as the temperature was raised, culminating in a density of 96.30 % at the maximum sintering temperature evaluated (1550 ℃) for $Ti_{16}Nb_2Sn$ [97].

Table 5.1. Compositions and densities of alloys.

Sample	Measured Density (g/cm^3)	Volumetric Porosity (%)
$Ti-18Nb$	4.01 ± 0.097	18.58
$Ti-18Nb-5Cu$	4.17 ± 0.067	17.48
$Ti-18Nb-7Cu$	4.22 ± 0.057	17.51
$Ti-18Nb-9Cu$	4.27 ± 0.072	17.59

On the other hand, compared to the reference material, porosity dropped upon the addition of Cu and then stayed essentially unchanged regardless of the amount of Cu added. This may be because the melting point of titanium copper alloys is reduced when copper is added [98].

5.2.2. XRD Analysis

XRD analysis was done to study the effect of the addition of copper on the phases formed in the microstructure, as shown in Figure 5.1. It is seen that the $Ti-Nb$ alloy consists of only α and $\beta-Ti$ phases. However, since it is difficult to detect a low amount of phases with general XRD analysis and the phase patterns of Nb and β–Ti is almost coincident (2θ degree; 38.3˚, 55.3˚, 69.3˚ and 82.1˚), they could not be identified and labeled. After the addition of Copper to the $Ti-18Nb$ alloy, the Ti_2Cu phase began to appear in the XRD analysis, and with increasing Cu addition, the amplitude of the peaks at 43.6˚ and 77.5˚ of this phase is seen according to JCPDS (standard card No. 14-0641) for Ti_2Cu phase. However, similar phases were detected in all Cu-added alloys. As shown by the binary phase diagram, the only stable phase that may occur in a $Ti-Cu$ alloy with less than 40% Cu is the Ti_2Cu phase [98]. The addition of less than 5 wt.% Cu to the $Ti-18\ Nb$ alloy results in the formation of the, and $\beta-Ti, the\ Ti_2Cu$ phase is produced, and the Ti_2Cu precipitates grow with increasing Cu content, as seen by the $Ti-Nb-Cu$ triple-phase diagram. According to this phase diagram, the structure is made up completely of $\beta-Ti\ and Ti_2Cu$ as the concentration of Cu increases. It's evidence that the Cu concentration allows for phase formation [98].

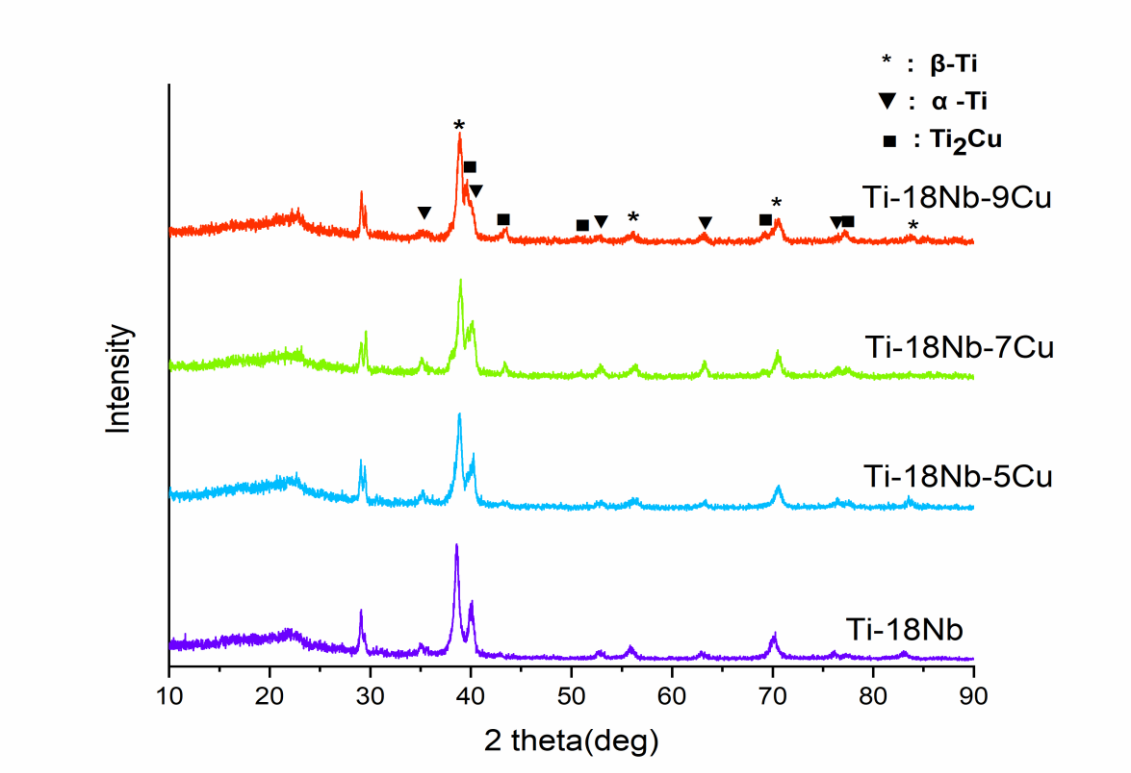

Figure 5.1. XRD analysis of prepared alloys.

5.2.3. SEM/EDS Analysis

The microstructure of Ti-18Nb alloy is depicted in Figure 5.2; it is composed of $\alpha - Ti$ and $\beta - Ti$ phases, as well as a trace quantity of undissolved Nb. However, the Ti-18Nb alloy does show signs of having certain Nb-rich areas. A lack of Ti may be seen in the white areas, while Nb in the light gray areas bordering this phase. Light gray areas can be found dispersed throughout the microstructure; however, whitish areas are rare. Sintering is aided by adding Cu, which explains why no Nb-rich regions exist in the alloys containing Cu.

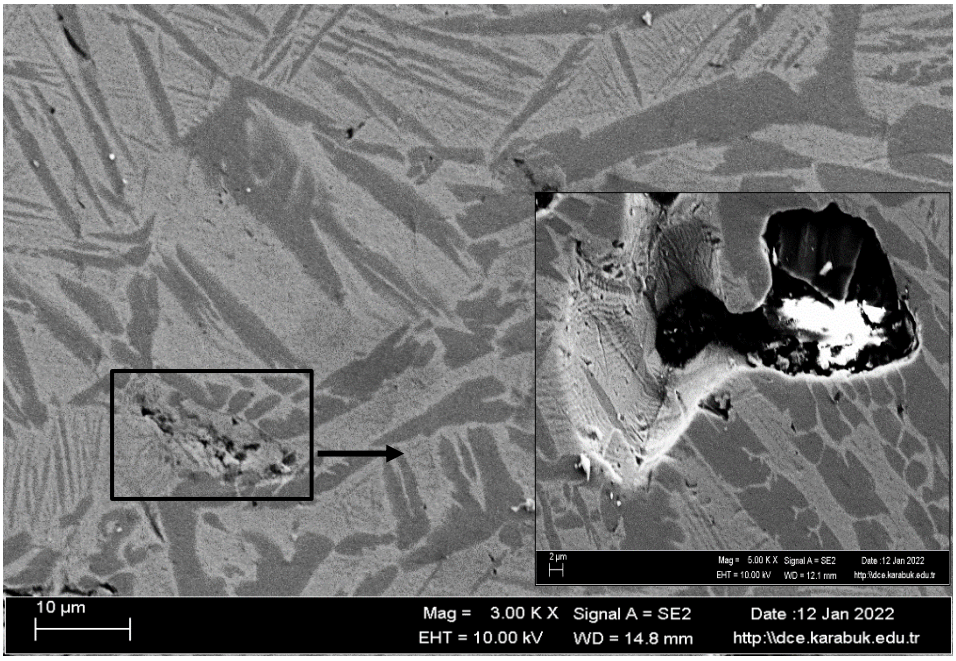

Figure 5.2. Microstructure of the $Ti-18Nb$ alloy.

It is the dissolving of Nb particles at about 900℃ that initiates the production of the $\beta\ -Ti$ structure in the general microstructure, the quantity of which rises with the increase in dissolved Nb [99]. Both Ti-10Nb and Ti-15Nb alloys showed the existence of Nb-rich phases up to 1100 ℃ when sintered from 900 ℃ to 1500 ℃. Furthermore, Martins et al. found that after sintering at 900°C, the form of these Nb-rich phases was irregular, but after sintering at 1100°C, the shape was spherical [100]. In comparison, Zhao et al. [101] reported an average sintering temperature of 1300°C to ensure complete homogeneity in Ti-Nb alloys. Based on our findings, Cu addition is compatible with homogenization and 1150°C.

Cu-added alloys uniformly have dark and bright regions in their microstructure. The amount of Nb increases in the light-colored regions and decreases in the dark regions (Figure 5.3 with line EDS). The areas with high concentrations of the β- stabilizer Nb are bright white, whereas the darker parts are known as $\alpha\ -Ti$. The $\alpha-phase$ or eutectoid transition with the dissolution of the β-Ti phase happened due to slow cooling in the furnace after sintering. Figure 5.3 shows the main β-Ti phases as the thick dark gray regions. No very fine phase development or martensitic transformation was detected, depending on the cooling rate.

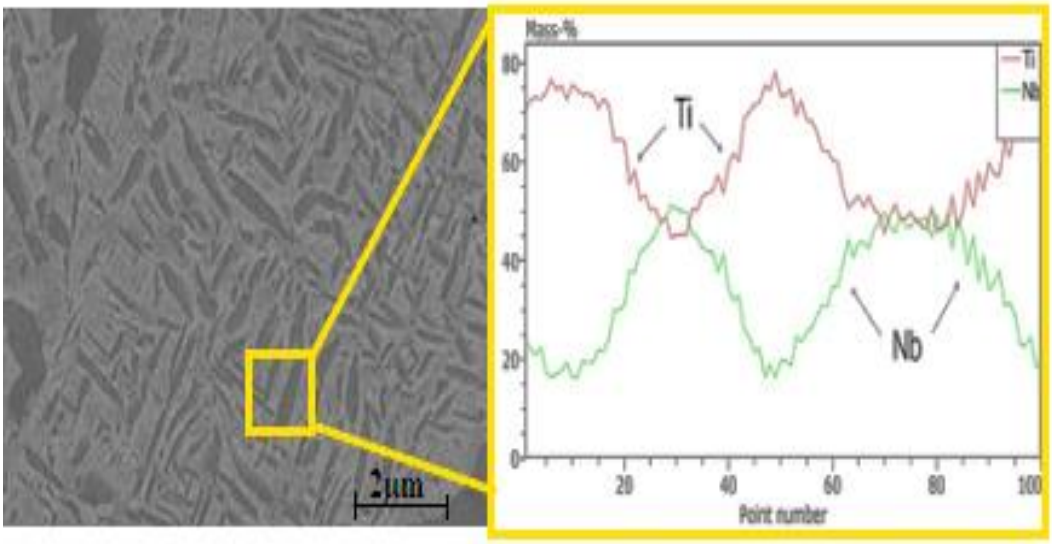

Figure 5.3. Microstructure of the $Ti-18Nb-7Cu$ alloy and line EDS analysis.

In addition to the generally similar microstructure in Copper-containing alloys, different colored (ash gray) phases were observed at the borders of the dark gray phases $(\alpha - Ti)$ in the alloy containing 9 wt.% Cu. This formation is generally determined in the full alloy microstructure Figure 5.4. In the point, EDS analyses made on the microstructure, analysis regions 4 and 8 belong to the β-Ti phase, while the other dark areas belong to the $\alpha - Ti$ phase. Unlike other alloys, the ash-gray regions 1, 3, and 7 formed in this microstructure show the Cu and Nb-rich parts of the $\alpha - Ti\ phase$. In the line EDS analysis of the specified region, it is seen that the amount of Nb is gradually increasing in this gray ash region formed after α-Ti, and the amount of Cu is higher than β-Ti, which is not seen in the other part of the α-Ti phase. Increasing the Cu amount led to diffuse Cu into α-Ti with thermal activation energy and forming a solid solution, thereby promoting the formation of α-Ti [102].

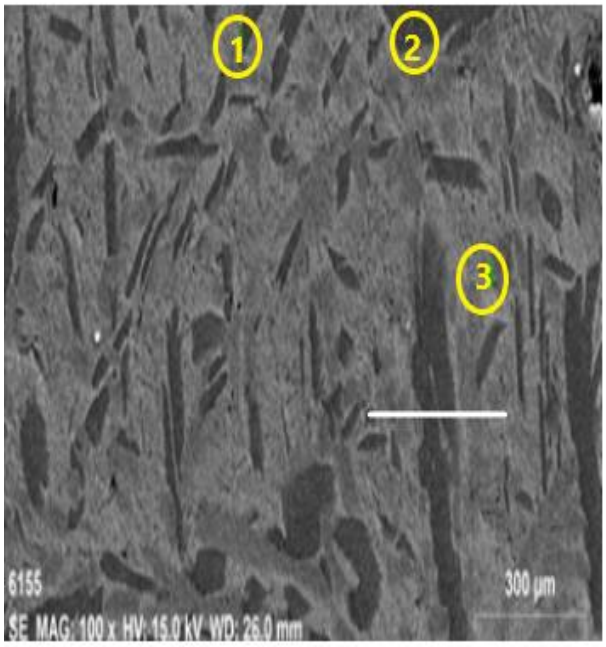

Mass percent (%)			
Spectrum	Ti	Cu	Nb
1	84.63	2.34	13.03
2	88.21	1.10	10.69
3	46.81	0.00	53.19

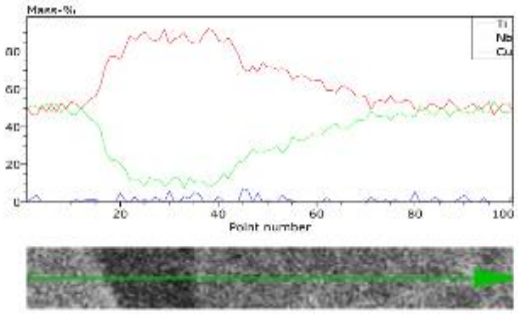

Figure 5.4. Microstructure of the Ti-18Nb-9Cu alloy and line EDS analysis.

5.2.4. AFM Analysis

The topography of a surface may be understood better with the use of atomic force microscopy (AFM) examination of individual profile lines (2D) or global profiles, extending the study to the surface (3D). When there are a lot of peaks and valleys in the photos, the arithmetic means height $(R\,a)$ and root-mean-square height $(R\,q)$ values are not as reliable as the average peak-to-valley difference (PVD) value.

Surface morphology for $Ti-18Nb-xCu$ alloys exhibits a distinct peak-to-valley difference at various length scales (from Figures 5.5 to 5.8), while the morphology of the base $Ti-18Nb\ alloy$ (Figure 5.5) has dimensions in the micrometer scale and a flat scan in the extracted profile due to the larger scale of the particles. The dimensions of the distance between objects are determined by the measurements of the surface's horizontal or lateral characteristics. Typically, characteristics like peaks and troughs make up a spacing parameter.

Pores, scratches, and small dimples were found by Vlcak et al. in their AFM analysis of the morphology of $Ti-Nb-Zr-Ta$ alloy; these features might be attributed to flaws that originate from the material's random heterogeneity [103].

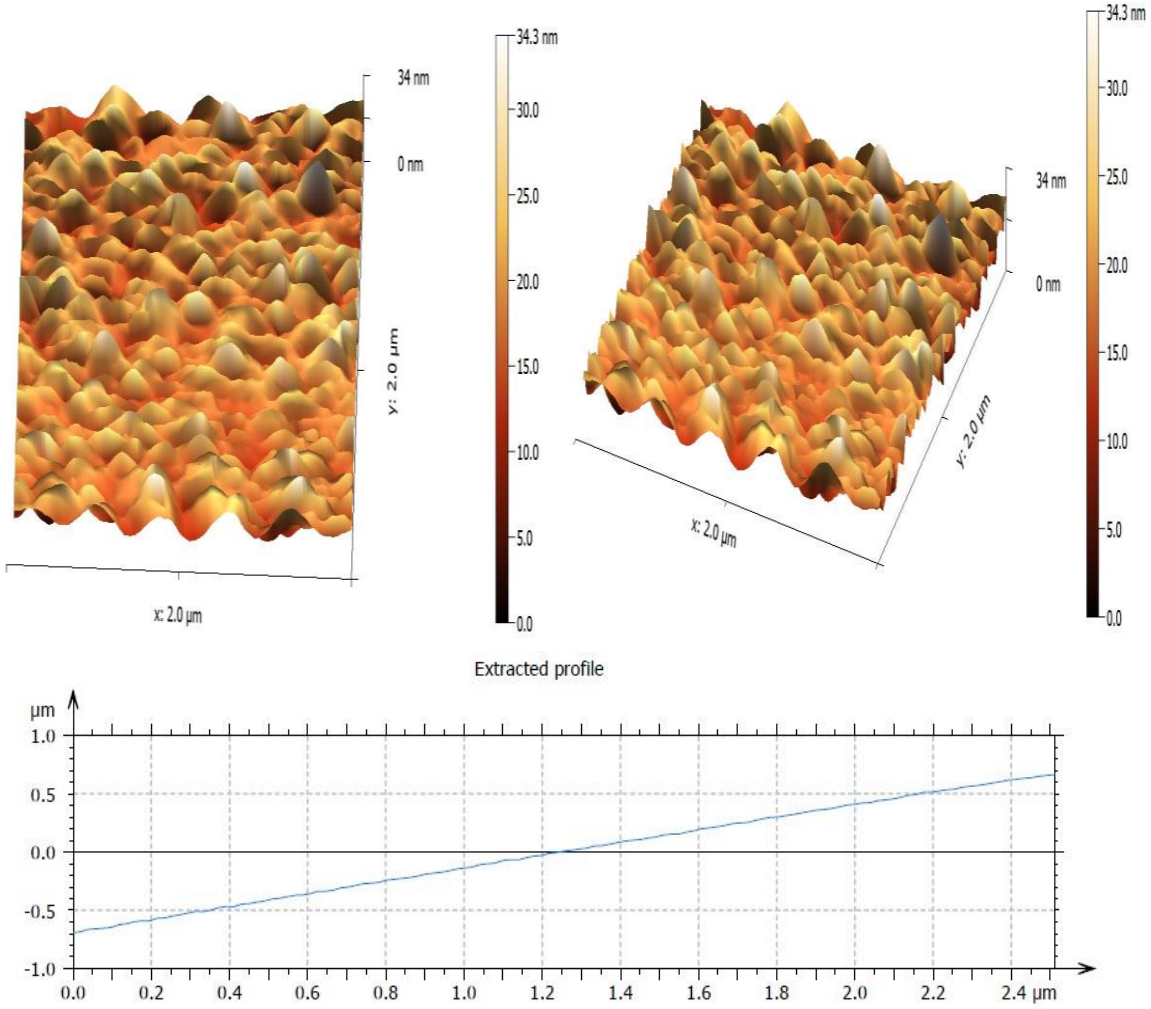

Figure 5.5. AFM analysis of $Ti-18Nb$ alloy.

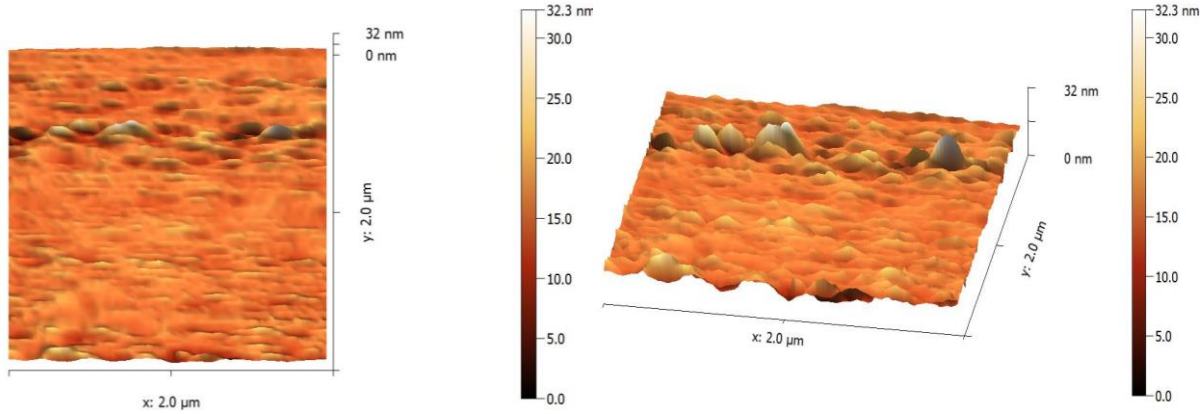

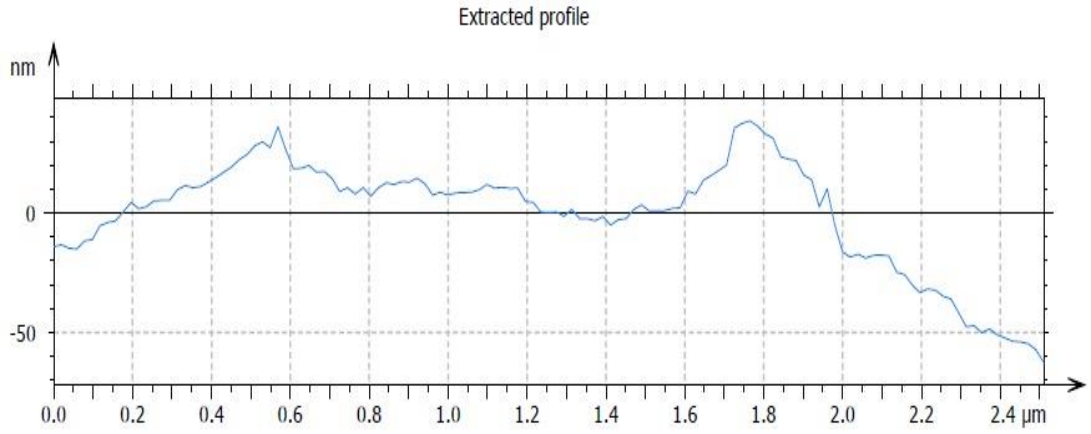

Figure 5.6. AFM analysis of $Ti-18Nb-5Cu$ alloy.

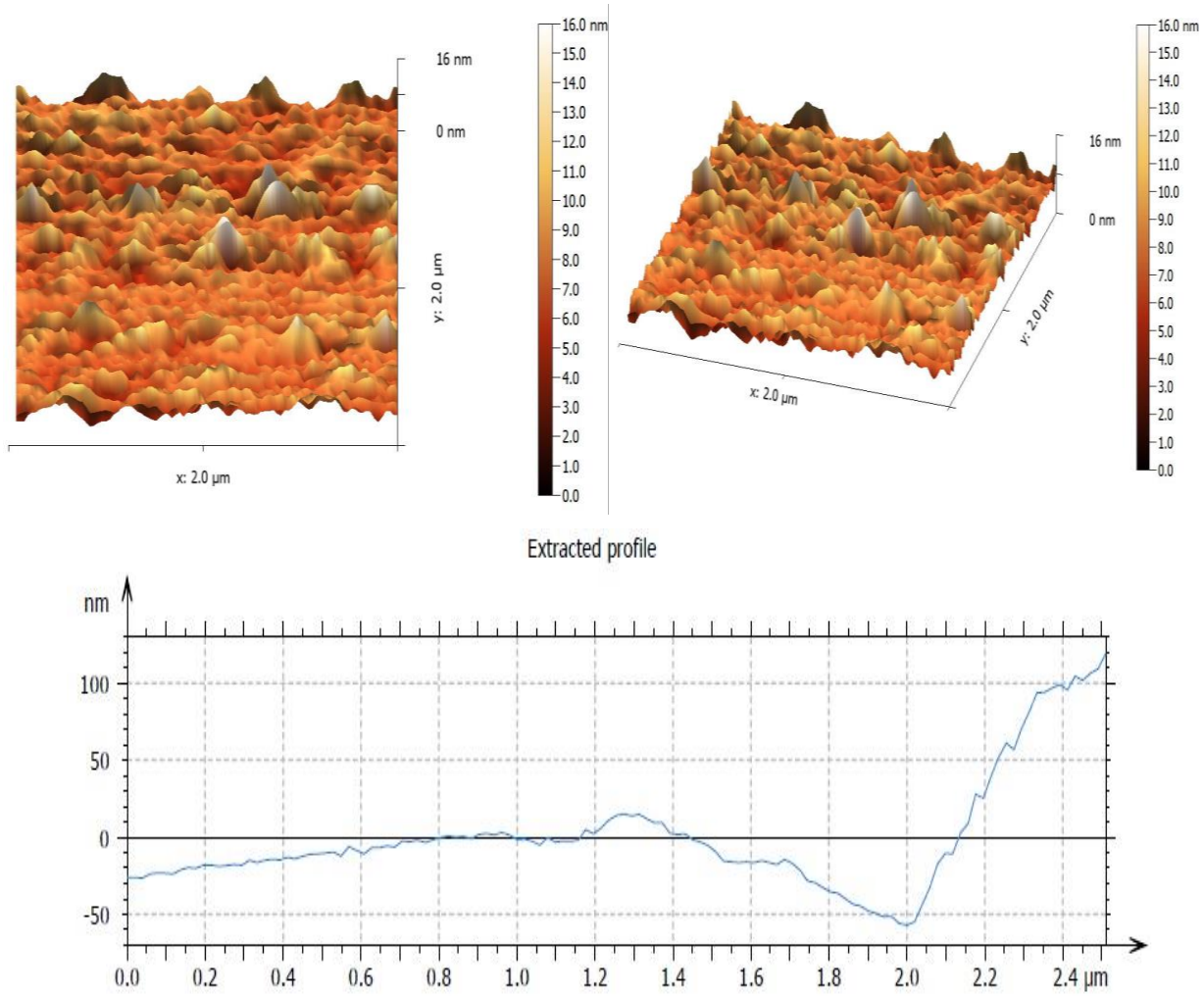

Figure 5.7. AFM analysis of $Ti-18Nb-7Cu$ alloy.

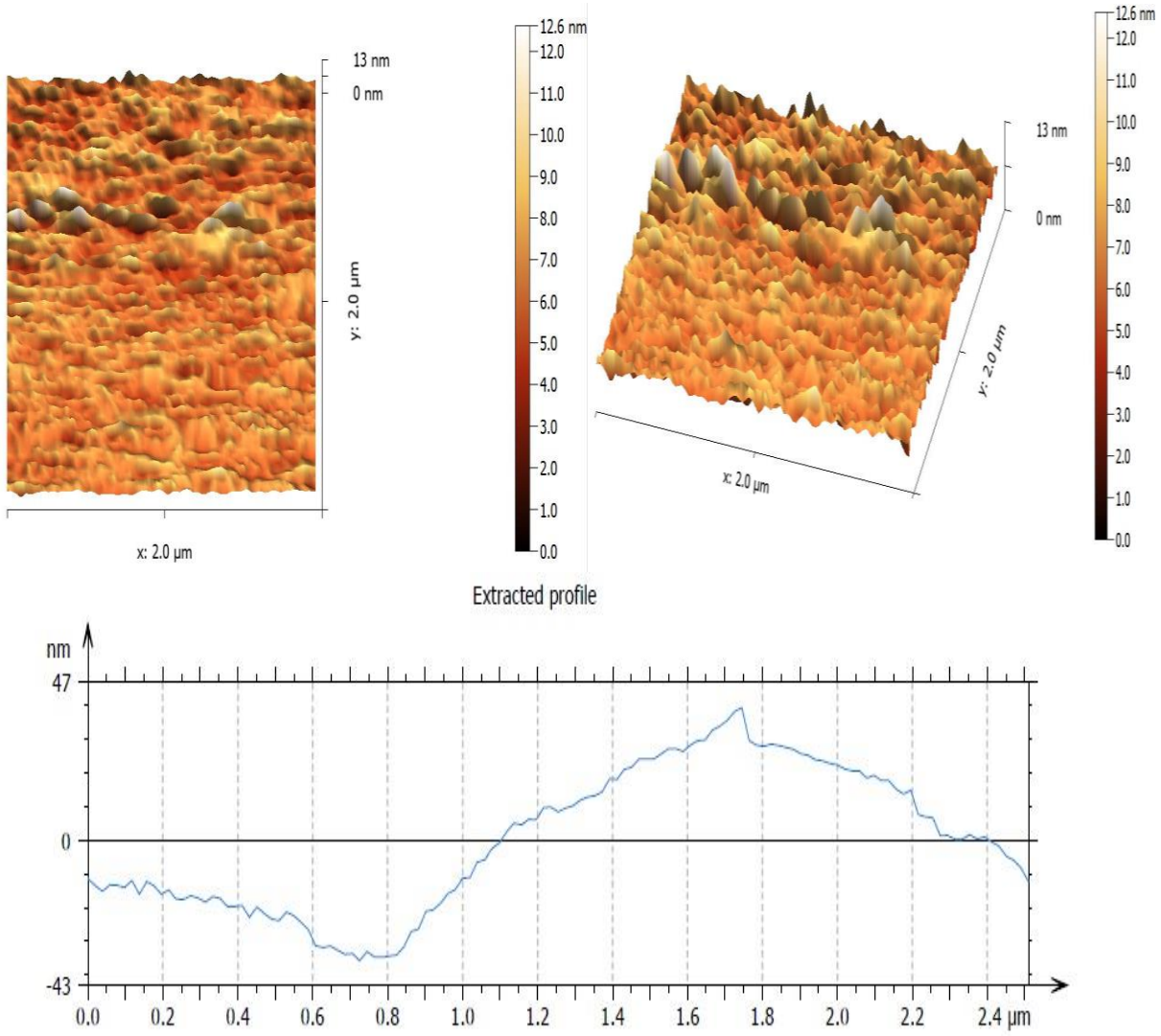

Figure 5.8. AFM analysis of $Ti-18Nb-9Cu$ alloy.

Table 5.2 lists the AFM analysis results and shows the R q. The $Ti-18Nb-9Cu$ alloy has the lowest value when Cu is added, and it also has the lowest interfacial area % (12.87 nm) and lowest surface roughness (12.87 nm). In order to properly analyze the interaction at the cell/implant interface, the cell size should be considered. It is well known that the roughness value strongly corresponds with the scanning size. According to many studies (osteoblast-like cells), orientation is strongly influenced by the surface shape, and these cells prefer rougher surfaces to smooth surfaces [104].

Table 5.2. AFM data of $TiNb$ alloys.

AFM Data	**Alloy**			
	$\boldsymbol{Ti-18Nb}$	$\boldsymbol{Ti-18Nb-5Cu}$	$\boldsymbol{Ti-18Nb-7Cu}$	$\boldsymbol{Ti-18Nb-9Cu}$
Root-mean-square height (Rq)	0.5444 μm	23.86 nm	29.41 nm	16.45 nm
Maximum height (Rz)	1.6630 μm	128.3 nm	191.4 nm	81.94 nm
Arithmetic mean height (Ra)	0.4874 μm	19.03 nm	20.06 nm	12.87 nm
Developed interfacial area ratio (Rdr)	39.81 %	1.881 %	2.095 %	0.7349 %

The Abbott-Firestone curve (Bearing area curve), which may mimic wear effects and provide information on the material and void volumes characterization, is a valuable tool for investigating surface morphology [105, 106]. The roughness of a bearing surface is measured in three dimensions, with the peak roughness corresponding to a height range of (2-25%) of the bearing length, the median roughness to (25-75%), and the valley roughness to (75-98%) [105]. ln accordance with the standard DIN 4776, which used the Abbott-Firestone curve's three-zone classification.

In other papers [107, 108], the Abbott-Firestone curve is divided into five intervals: 5%, 5%, 10%, 50%, 95%, and 99%. These findings can be applied to the study of porous surfaces; the first zone comprises extremely high and noticeable asperities that undergo wear; the second zone comprises bearing and fluid retention capabilities, also called microroughness; and the third zone comprises a relatively smooth surface that is resistant to wear. The fourth zone describes the surface's voids or pores, while the fifth zone's depth may be used as a measure of the surface's load capacity and wear resistance.

Figure 5.9 shows the Abbott-Firestone curve for all prepared alloys indicating that the Ti-18Nb (without the addition of Cu) has heights ≤5% that are more liable to wear, while the addition of Cu with different concentrations gives curves have heights in the range of 10–50% that have retention capabilities and maybe suffer from microroughness. However, it is clear from the surface profile that the alloy with 7wt% Cu has the lowest theoretical wear rate (see Figure 5.10).

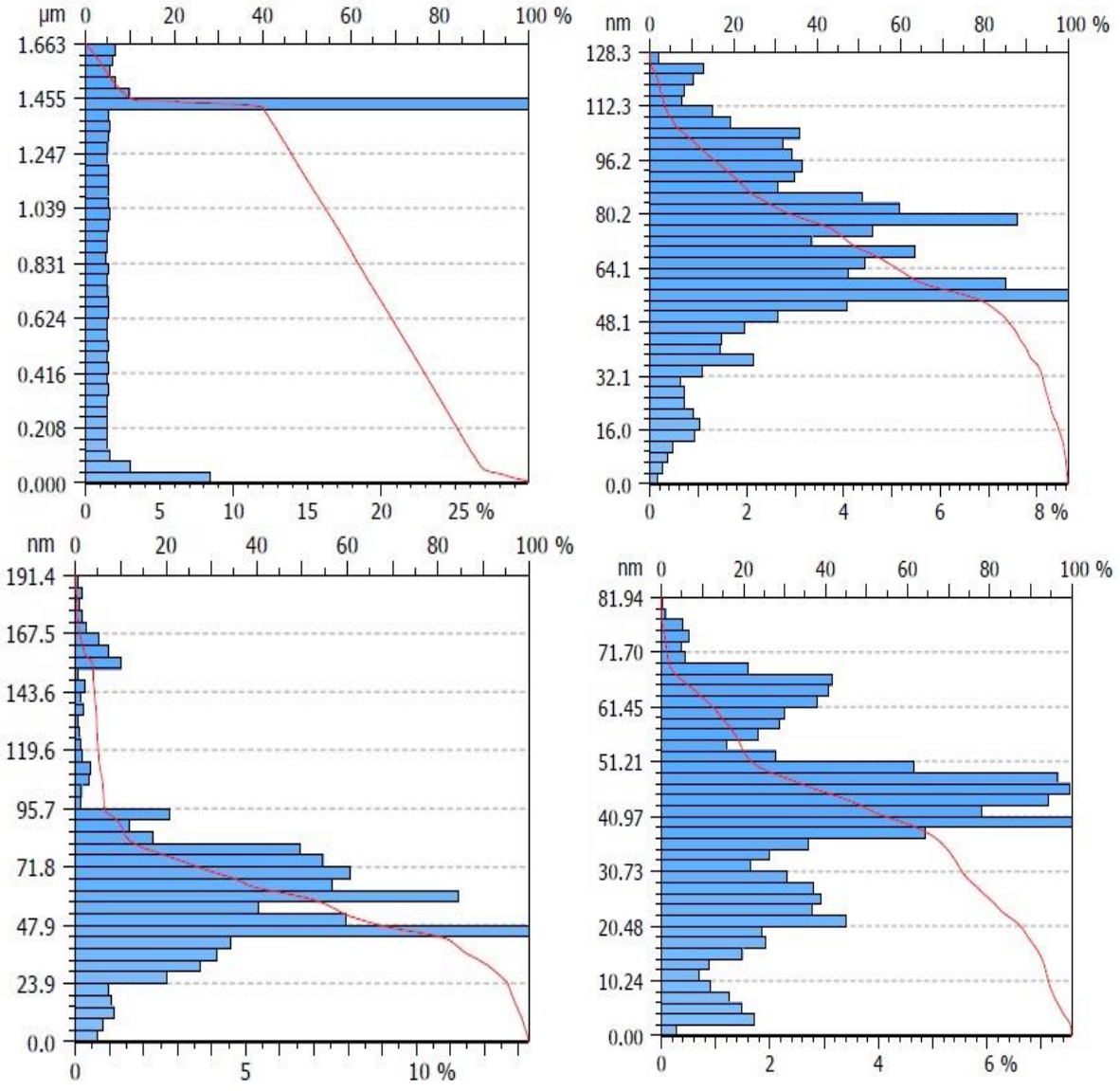

Figure 5.9. Abbott-Firestone curve for Ti-18Nb-xCu alloy.

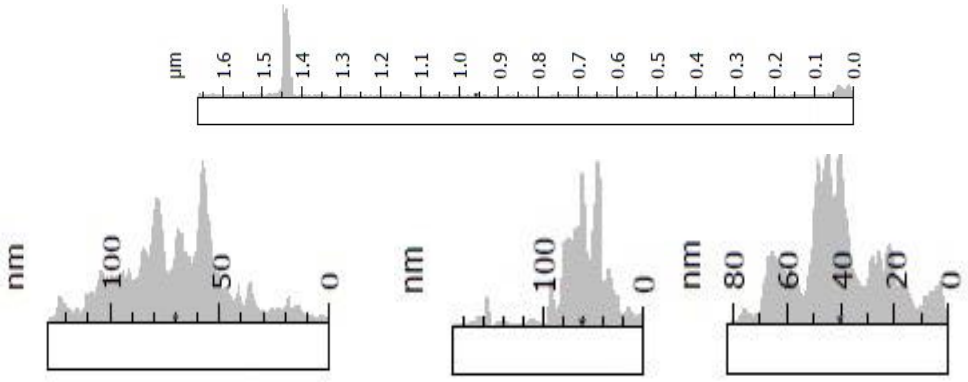

5.10 Profile of alloy surface.

5.3 DRY WEAR RATE

Sliding dry wear tests were performed with loads of 5, 10, and 15 N for a set period (10 min). As shown in Figure 5.11 and Table 5.3, the wear rate (W.R) rises with increasing load for all alloys. However, under constant load, the wear rate is lower $for\ Ti-18Nb$ alloys with Cu addition compared to those without addition. This is because the Ti_2Cu phase, as shown by the XRD study, develops a stable phase with the addition of Cu, which may result in a more rigid alloy. $Ti-18Nb-7Cu$ alloy had the lowest wear rate value because the solid solution strengthened in the -Ti phase and precipitated the Ti_2Cu phase [109]. However, Ilven et al., who developed a β-type Ti-35Nb-10Cu alloy, elaborated on how Cu addition improves sinterability and provides precipitation hardening capability [110]. The AFM study shows that the maximum surface roughness for Ti-18Nb-7Cu alloy offers more significant hardening, increasing wear resistance and making the wear process more difficult.

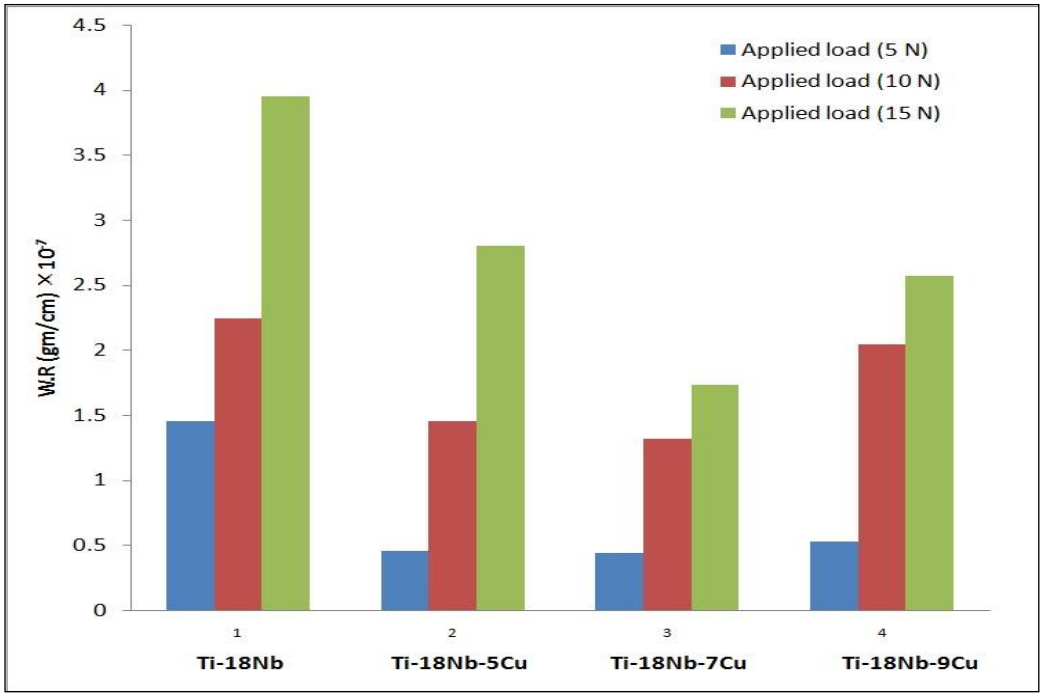

Figure 5.11. Wear rate comparison for alloys.

Table 5.3. Wear rate values at different applied loads and constant time.

Alloy	W.R (gm/cm) $\times 10^{-7}$		
	5 N	10 N	15 N
Ti-18Nb	1.4485	2.2434	3.9481
Ti-18Nb-5Cu	0.4516	1.4485	2.7999
Ti-18Nb-7Cu	0.4393	1.3160	1.7311
Ti-18Nb-9Cu	0.5265	2.0403	2.5702

5.4. CORROSION BEHAVIOR

Metals have high mechanical qualities, but they may be damaged by electrochemical assault, meaning that they can corrode or wear down, releasing particles that can irritate the human body's environment and trigger local and systemic biological reactions. Titanium and its alloys have the highest corrosion resistance of any biomaterial, and some β-Ti alloys provide sufficient strength and corrosion resistance; these include $Ti-5Al-5Fe, Ti-6Al-4V, and\ Ti-6Al-7Nb,$ etc.; however, the aluminum in these alloys has been linked to bone diseases and neurological disorders. Titanium alloys' primary drawbacks are their poor wear qualities, high cost, and oxygen penetration during manufacture and heat treatment, which causes embrittlement of titanium and the localized breakup of the extremely passive coating. Corrosion of manufactured Ti-18Nb alloys studied in 37°C body-fluid models. First, as seen in Figure 5.12, when potential-time measurements (OCP) are taken over 3600 seconds, the low amount of copper (5 wt% Cu) causes fluctuation in potentials with the time that started with a quick decline followed by semistable behavior. An AFM's analysis of the surface roughness suggests that the low % of $Cu\ in\ Ti-18Nb$ alloy may have surface irregularities. Since copper has a positive potential of +0.337 V, it acts as a promising cathode and results in the formation of the Ti_2Cu phase. Stability improvements were seen at addition levels of 7 and 9 wt%.

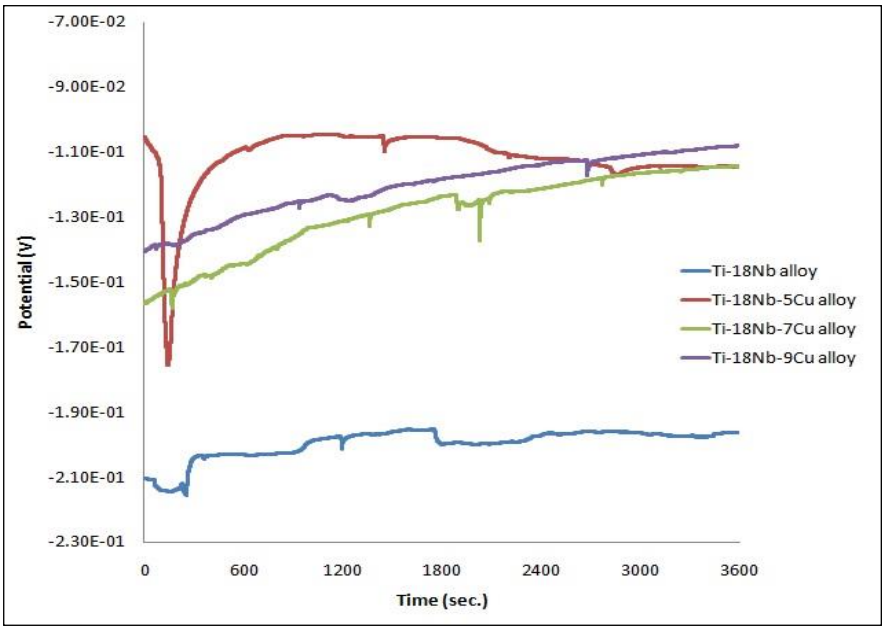

Figure 5.12. Potential – time measurements.

Second, the polarization curves of Ti-18Nb-xCu alloys in Figure 5.13 indicate cathodic and anodic areas, and the most effective processes that take place at electrodes are shown in Figure 5.14:

$$Ti \rightarrow Ti^{4+} + 4e \quad (5.1)$$

$$Ti^{4+} + 2H2O \rightarrow [Ti(OH)2]^{2+} + 2H^{+} \quad (5.2)$$

$$Ti^{4+} + 4H2O \rightarrow Ti(OH)4 + 4H^{+} \quad (5.3)$$

The following oxygen reduction processes are possible at the cathodic site:

$$O_2 + 4e + 2H_2O \rightarrow 4OH^{-} \quad (5.4)$$

Ti-18Nb-5Cu alloy's polarization curve changed toward higher current density values, indicating a faster corrosion rate. $Ti-18Nb-7Cu$ *and* $Ti-18Nb-9Cu$ alloys exhibited polarization curve behavior comparable to that of $Ti-18Nb$ alloy at higher noble potentials.

Compared to CP-Ti, the OCP curves shown by the Ti16Nb alloy in the research by Wang and Zheng were relatively stable. Furthermore, the oxide coating on Ti-16Nb alloy, mainly consisting of TiO_2 and Nb_2O_5, provided superior corrosion resistance than CP-Ti because it acted as a barrier to the released interior metal ions [111].

While another work by Mutlu and Oktay showed how a $Ti-Nb-Cu$ alloy's polarization resistance decreased as Cu content increased, the latter demonstrated how a passive oxide coating acted as a barrier to electrochemical corrosion and improved

the surface's resistance to charge transfer. However, the formation of the Ti_2Cu phase with increased Cu concentration accelerates corrosion [112]. Furthermore, Mutlu et al. argued that increasing the Copper content of $Ti-Nb-Cu$ alloys reduces the corrosion potential and increases the corrosion current density [110].

Table 5.4 displays the corrosion behavior data; the addition of Copper to $Ti-18Nb$ alloy raised the corrosion potential (Ecorr), and the change of Cu content in the alloy influenced the corrosion current density (Icorr), with the lowest (Icorr) being for $Ti-18Nb-9Cu$ alloy.

Changes in the surface's redox reactions also led to shifts in the cathodic and anodic Tafel slopes. The hydrogen evolution process may combine with the lattice structure of some metals, leading to embrittlement, and is a frequent cathodic reaction in almost corrosive conditions for metals. Table 5.4 shows that, on average, cathodic Tafel slopes are more significant than would be predicted by the Volmer-Tafel mechanism (bc=0.120 $V.dec^{-1}$). This indicates that film formation affects the reduction reaction by acting as a barrier for charge transfer at the film formed or by controlling the energy of the reaction itself at the double layer, or both. Hydrogen molecules evolving on the oxide-covered electrode may function as charge carriers ($H3O^+$ ions) or as electrons that operate as an energy barrier for the oxide layer reaching the oxide/solution interface, where neutralization occurs between each two charge carriers (i.e., $H3O^+$ and e). This structure represents a "Dual-barrier model" [113]. Specifically, the process is neither a chemical desorption step in which the adsorbed H atom diffuses over the metal surface and produces a cathodic slope smaller than (0.120 $V.dec^{-1}$) nor an electrochemical desorption step in which the cathodic slope is produced (-0.05 $V.dec^{-1}$).

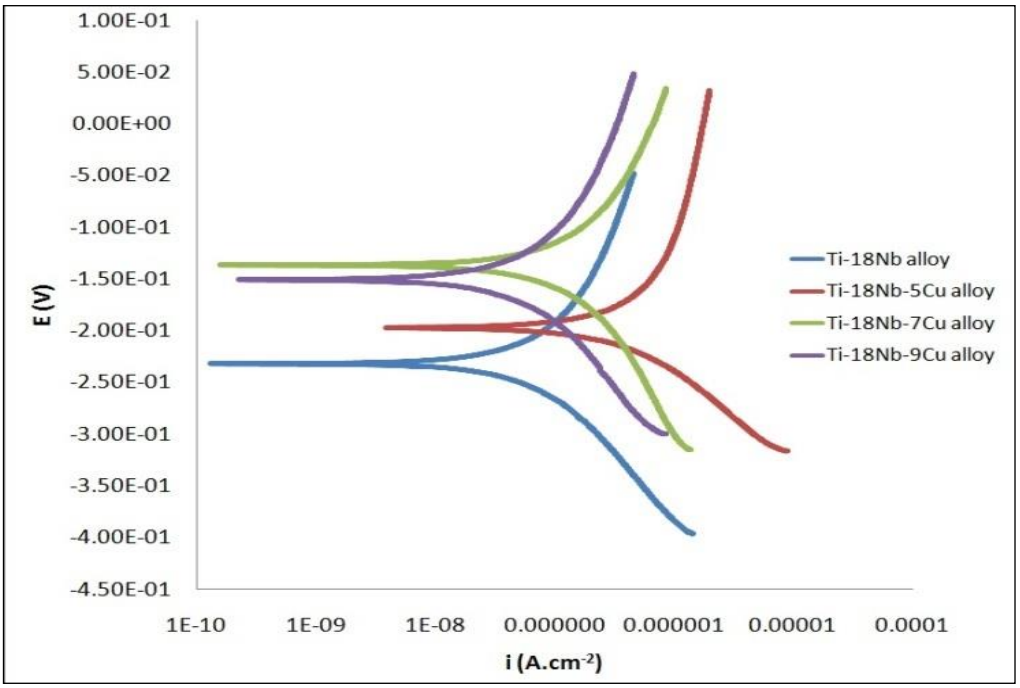

Figure 5.13. Polarization curves of $Ti-18Nb-xCu$ alloys.

The following equation may be used to calculate the corrosion rate (C.R.) in mil per year utilizing corrosion current densities and equivalent weight e and density of alloys:

$$C_R = 0.13 \times i_{corr}\left(\frac{e}{\rho}\right) \qquad (5.5)$$

Table 5.4 demonstrates that the incorporation of copper led to an increase in the rate of dissolution, and this finding is in line with the findings of Cheng et al., who demonstrated that the formation of a lamellar Ti_2Cuphase lowers the corrosion resistance of the material, causes the formation of micro-galvanic cells within the matrix, and raises the value of the galvanic driving force (V) at the $Ti_2Cu/\alpha - T$ [104]. They also simplified the complicated anodic dissolution of Ti_2Cu in a biologically relevant simulated fluid as:

$Ti_2Cu + 8OH^- \rightarrow 2TiO_2 + Cu^{2+} + 4H_2O + 10e$ (5.6)

Firstly, Ti_2Cu converts to Ti^{4+} and Cu^{2+} [14, 114][14, 114], followed by converting Ti^{4+} and OH^- to TiO_2

Polarization resistance $(R.P.)$ also can be calculated using Tafel slopes $(bc$ & $ba)$ and current densities as follow:

$$R_p = \frac{b_c \times b_a}{2.303 \times i_{corr}(b_c + b_a)} \qquad (5.7)$$

The lowest interfacial area ratio (Rdr) from AFM data for this alloy may explain why it has more excellent resistance than another alloy, according to (R.P.), as it reduces

the number of micro-galvanic cells generated.

Table 5.4 Corrosion data of $Ti-18Nb-xCu$ alloy in SBF at 37°C.

Data	Alloy			
	$Ti-18Nb$	$Ti-18Nb-5Cu$	$Ti-18Nb-5Cu$	$Ti-18Nb-5Cu$
$-E_{corr}$ (V)	0.232	0.197	0.137	0.151
i_{corr} $(A.cm^{-2}) \times 10^{-7}$	1.284	8.028	2.434	1.230
$-b_c$ $(V.dec^{-1})$	0.1733	0.1278	0.3258	0.2077
$+b_a$ $(V.dec^{-1})$	0.3144	0.5535	0.3734	0.3271
C_R $(mpy) \times 10^{-8}$	4.287	29.116	9.108	4.745
R_P $(k\Omega.cm^2)$	377.81	56.158	310.39	448.46

In contrast to the cyclic curve for Ti-18Nb alloy, Figure 5.14 illustrates the cyclic polarization for produced alloys, demonstrating curves shifting after adding copper to larger current densities. Despite the breakdown potential (Ebd) for the $Ti-18Nb-5Cu, Ti-18Nb-7Cu, and\ Ti-18Nb-9Cu$ alloys rising in the presence of Cu in the base alloy to 0.156, 0.167, and 0.172 V, respectively, as compared to the Ti-18Nb alloy (0.0617 V), the behavior indicates an increased propensity for pitting.

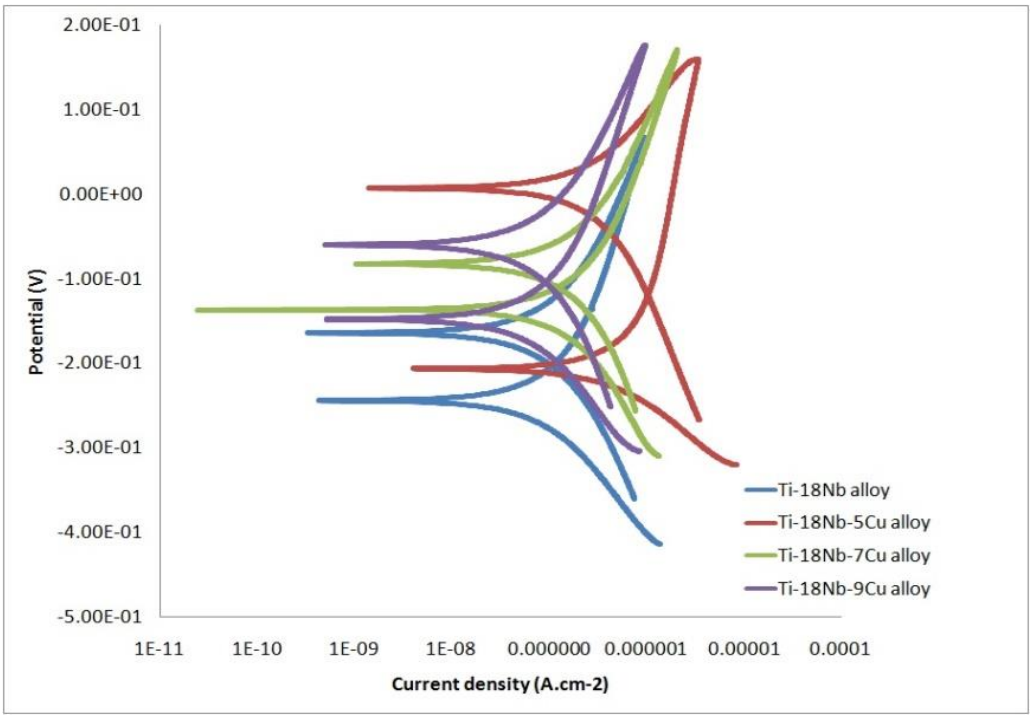

Figure 5.14. Cyclic polarization of prepared alloys in SBF at 37°C.

SEM has been used to analyze the microstructure of the corroded surface in order to evaluate the impact of corrosion on the alloy's surface. Figure 5.15 SEM for specimen

after corrosion for $Ti-18Nb-xCu$ in Ringer's solution shows that the color of the surface has changed due to the corrosion products, and from that color, it can be estimated that the corrosion has occurred on the surface. Focused on the pits that appeared on the surface, primarily in pores areas due to corrosion because the pores represent a point defect that can be the direct cause. The localized corrosion was created after the electrochemical test despite the surface having passive layers like TiO_2 and Nb_2O_5, and damage may happen at the Ti_2Cu/Ti contact, as shown by SEM images for alloys following corrosion in Figure 5.15.

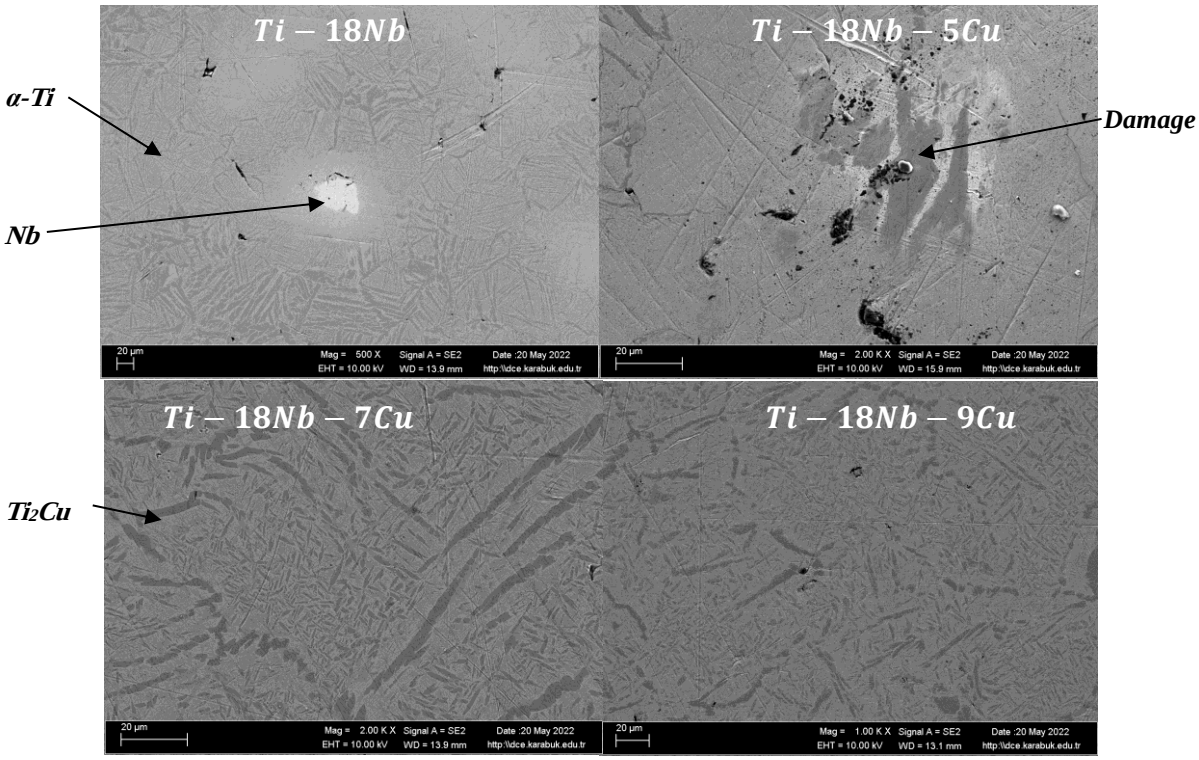

Figure 5.15. SEM images of $Ti-18Nb-xCu$ alloys after corrosion test.

5.5. ANTIBACTERIAL TEST

As shown by Erlin et al. when they examined the antibacterial property of the Ti-Cu sample, Figure 5.15 depicts the inhibition zones around Ti-18Nb-xCu alloys against Escherichia coli exhibit no inhibition zone after adding Cu to base alloy [115]. The Ti-10Cu alloy, on the other hand, was shown by Xiaoyan et al. to kill bacteria quickly (1 day) after implantation and virtually completely (4 days) afterward, but the CP-Ti was unable to perform this function [116]. Also, the antibacterial solid Ti-Cu alloy was investigated by Moniri et al. [117]. Numerous prior research has examined the

antibacterial activity of metallic implants, including copper, copper alloys, copper-modified surfaces, and copper-containing alloys. These studies found that the release of Cu(2+) is the primary cause of these implants' antibacterial capabilities [49, 118]; when the released Cu(2+) comes into touch with the bacterial outer membrane during nutritional supplementation or due to electrostatic pressures on the bacterial surface. Additionally, the migration of Cu(2+) into the cell would result in the production of intercellular reactive oxygen species (ROSs), including superoxide radical anion (O=), hydrogen peroxide (H_2O_2), and extremely reactive hydroxyl radicals (OH). When these highly reactive species interact with physiologically significant molecules like lipids, proteins, and nucleic acids, the result is oxidative damage or the organism's death [119].

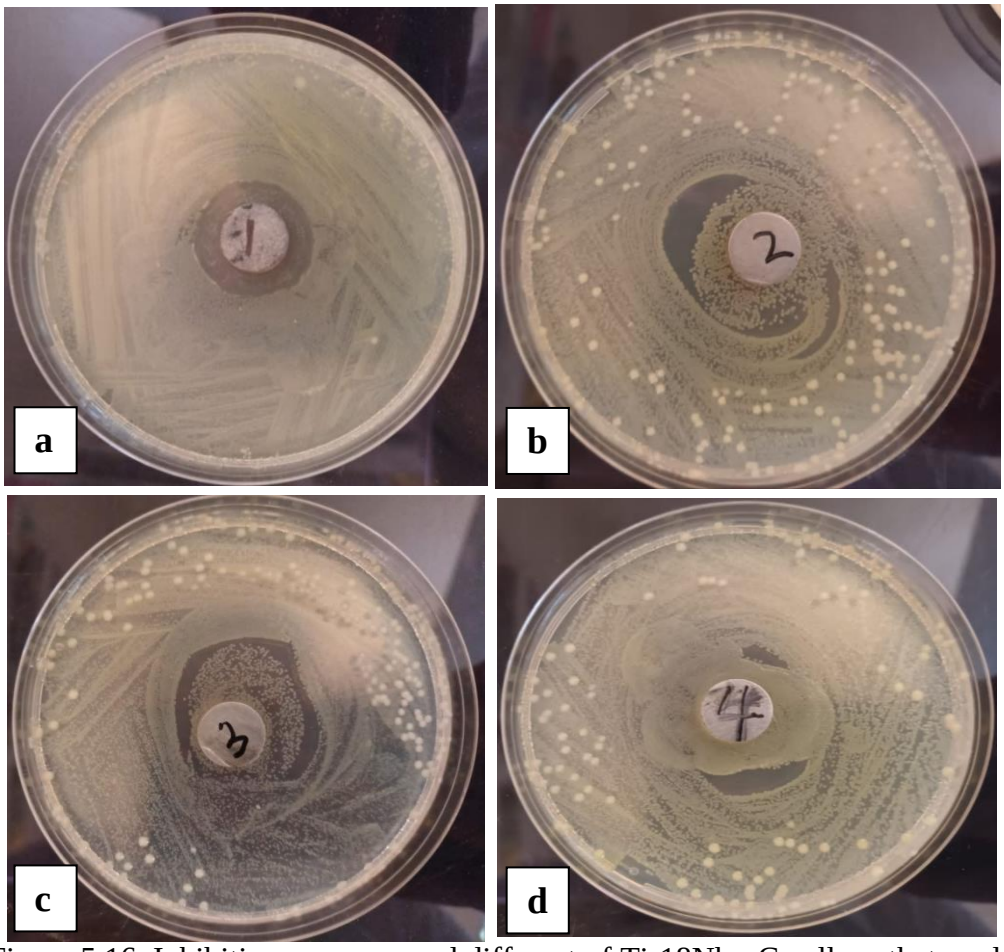

Figure 5.16. Inhibition zones around different of Ti-18Nb-xCu alloys that are labeled as (a) $Ti-18Nb$, (b) $Ti-18Nb-5Cu$, (c) $Ti-18Nb-7Cu$ and (d) $Ti-18Nb-9Cu$ alloy.

PART 6

CONCLUSIONS AND RECOMMENDATION

6.1 CONCLUSIONS

In this work, the transformations of phases, mechanical properties, and corrosion resistance of alloys of the Ti-18Nb and Ti-18Nb-XCu system were investigated, and the results obtained allow us to state the following conclusions:

i. Ti-18Nb and Ti-18Nb-XCu alloy was prepared with different addition ratios of copper by powder metallurgy (P/M) method.

ii. Analysis by XRD shows that the prepared alloys have α and β phases structure with $CuTi_2$ compound appearing; in addition, a proportion of Cu is present in the alloy.

iii. The density increases with the increase of the copper content. It was in the range (of 4.01-4.27 g/cm^3), while the porosity decreased when copper content rose, whose values were within (18-58-17.59 %).

iv. Due to the enhancement of the Ti_2Cu phase, which occurs in 7 wt%, AFM results showed that the Ti-18Nb-7Cu alloy had the largest peaks, roughness, and interfacial area.

v. Because $Ti-18Nb-7Cu$ alloy is the hardest sample, the wear rate under three loads at a constant time was the lowest for this material.

vi. Due to the behavior of copper as an effective cathodic region and the existence of the Ti_2Cu/Ti interface, which accelerates the galvanic cells, the inclusion of Cu in the basic $Ti-18Nb$ alloy had an impact on the corrosion characteristics.

6.2 RECOMMENDATIONS

The results obtained in the course of this investigation allow us to suggest the continuation of studies through the following lines of complementary research:

i. To study the effect of Cu addition on the martensitic structure of $Ti-18Nb$ alloy and its influence on corrosion resistance and mechanical properties.
ii. Evaluate the effect of shape memory and corrosion fatigue of the Ti-18Nb-XCu alloy.
iii. Change the proportion of the mixture and carry out new tests to expand the knowledge and application of this promising alloy.
iv. Carry out the sintering process using different temperatures and atmospheres, obtaining interesting results.
v. Fabricate and implant animal samples for Ti-18Nb-XCu alloy biocompatibility testing, paving the way for possible future human implants.

REFERENCES

1. Li, H., et al., "*Production of Ti–13Nb–13Zr alloy by powder metallurgy (P/M) via sintering hydrides"*. **Materials Manufacturing Processes.** 31(6): 719-724 (2016)

2. Brånemark, P.-I., et al., "*Intra-osseous anchorage of dental prostheses: I. Experimental studies."* **Scandinavian journal of plastic reconstructive surgery** , 3(2):81-100(1969)

3. Niinomi, M., et al., "*Biomedical titanium alloys with Young's moduli close to that of cortical bone."* **Regenerative biomaterials**, 3(3):173-185 (2016)

4. Zhang, L.-b ،.et al., "*Effect of Nb addition on microstructure, mechanical properties and castability of β-type Ti–Mo alloys"*. **Transactions of Nonferrous Metals Society of China**, 25(7):2214-2220.(2015)

5. Stráský, J., et al., "*Increasing strength of a biomedical Ti-Nb-Ta-Zr alloy by alloying with Fe, Si and O"*. **Journal of the mechanical behavior of biomedical materials**, 71:329-336.(2017)

6. Garellick, G., et al., "*Swedish hip arthroplasty register: annual report"*. **Department of Orthopaedics, Sahlgrenska University Hospital**.(2009) ،

7. Klevens, R.J., "*Active bacterial core surveillance (ABCs) MRSA investigators. Invasive methicillin-resistant Staphylococcus aureus infections in the United States"*. **Jama**, 298:1763-1771.(2007)

8. Gill, S.R., et al., "*Insights on evolution of virulence and resistance from the complete genome analysis of an early methicillin-resistant Staphylococcus aureus strain and a biofilm-producing methicillin-resistant Staphylococcus epidermidis strain"*. **Journal of bacteriology**, 187(7):2426-243.(2005) 8

9. Unosson, E., et al., "*In vitro antibacterial properties and UV induced response from Staphylococcus epidermidis on Ag/Ti oxide thin films"*. **Journal of Materials Science: Materials in Medicine**, 27(3):1-8.(2016)

10. Cao, Y. et al., "*Nanostructured titanium surfaces exhibit recalcitrance towards Staphylococcus epidermidis biofilm formation"*. **Scientific reports**, 8(1):1-13 .(2018)

11. Velasco, S.C., A. Cavaleiro, and S.J. Carvalho, "*Functional properties of ceramic-Ag nanocomposite coatings produced by magnetron sputtering"*. **Progress in Materials Science**, 84:158-191.(2016)

12. Marković, D., et al., "*Novel antimicrobial nanocomposite based on polypropylene non-woven fabric, biopolymer alginate and copper oxides nanoparticles"*. **Applied Surface Science**, 527:146829.(2020)

13. Wang, M. and T.J. Tang, "*Surface treatment strategies to combat implant-related infection from the beginning"*. **Journal of orthopaedic translation**, 43: 17-54 (2019).

14. Zhang, E., et al., "*Antibacterial metals and alloys for potential biomedical implants"*. **Bioactive materials**, 6(8):2569-2612.(2021)

15. Lu, M., et al., "*Enhanced antibacterial activity of Ti-Cu alloy by selective acid etching"*. **Surface Coatings Technology**,421:127478 (2021).

16. Amin, A.N., *Titanium Alloys* :*Towards Achieving Enhanced Properties for Diversified Applications*. 2012: BoD–Books on Demand.

17. Oldani, C. and A.J.R.a.i.a. Dominguez, "*Titanium as a Biomaterial for Implants"*. **Recent advances in arthroplasty**, 149:162-218 (2012).

18. Niinomi, M. and C.J. Boehlert, *Titanium alloys for biomedical applications*, in *Advances in metallic biomaterials*. 2015, Springer. p. 179-213.

19. Okazaki, Y., et al., "*Corrosion resistance, mechanical properties, corrosion fatigue strength and cytocompatibility of new Ti alloys without Al and V"*. **Biomaterials**, 19(13):1197-1215.(1998)

20. Gordin, D. et al., "*WITHDRAWN: synthesis, structure and electrochemical behavior of a beta Ti–12Mo–5Ta alloy as new biomaterial"*. **Materials letters**, 59(23):2959-2964.(2005)

21. Godley, R., D. Starosvetsky, and I.J.J.o.M.S.M.i.M. Gotman, "*Corrosion behavior of a low modulus β-Ti-45% Nb alloy for use in medical implants"*. 17(1):63-67.(2006)

22. Assis, S.L.d., et al., "*A comparative study of the in vitro corrosion behavior and cytotoxicity of a superferritic stainless steel, a Ti-13Nb-13Zr alloy, and an austenitic stainless steel in Hank's solution"*. 73(1):109-116.(2005)

23. Martins, D.Q., et al., "*Effects of Zr content on microstructure and corrosion resistance of Ti–30Nb–Zr casting alloys for biomedical applications"*. **Electrochimica Acta**, 53(6):2809-2817.(2008)

24. Debelian, G. and M.J. Trope, "*The use of premixed bioceramic materials in endodontics"*. **Giornale italiano di endodonzia**, 30(2):70-80.(2016)

25. Wang, B., Y. Zheng ،and L.J. Zhao, "*Effects of Sn content on the microstructure, phase constitution and shape memory effect of Ti–Nb–Sn alloys"*. **Materials Science Engineering: A**, 486 (1-2):146-151 (2008).

26. Cvijović-Alagić, I. et al., "*Wear and corrosion behaviour of Ti–13Nb–13Zr and Ti–6Al–4V alloys in simulated physiological solution*". **Corrosion Science**, 53(2):796-808.(2011)

27. Guo, Y.-y., et al., "*In vitro corrosion resistance and cytotoxicity of novel TiNbTaZr alloy*". **Transactions of Nonferrous Metals Society of China**, 22:s175-s180.(2012)

28. Ribeiro, A.L.R., et al., "*Are new TiNbZr alloys potential substitutes of the Ti6Al4V alloy for dental applications? An electrochemical corrosion study*". **Biomedical Materials**,8(6): 065005 (2013).

29. Calderon-Moreno, J.M., et al., "*Microstructural and mechanical properties, surface and electrochemical characterisation of a new Ti–Zr–Nb alloy for implant applications*". **Journal of alloys compounds**, 398:410-612 (2014)

30. Liu, X., et al., "*Cytocompatibility and early osseointegration of nanoTiO2-modified Ti-24 Nb-4 Zr-7.9 Sn surfaces*". **Materials Science Engineering: C**,256:48-262 (2015).

31. Wang, Z., et al., "*Micro-abrasion–corrosion behaviour of a biomedical Ti–25Nb–3Mo–3Zr–2Sn alloy in simulated physiological fluid*". **Journal of the Mechanical Behavior of Biomedical Materials**, 63:361-374.(2016)

32. Correa, D., et al., "*Development of Ti-15Zr-Mo alloys for applying as implantable biomedical devices*". **Journal of Alloys Compounds**, 163:171-749 (2018).

33. Bao, M., et al., "*Tribocorrosion behavior of ti–cu alloy in hank's solution for biomedical application*". **Journal of Bio-and Tribo-Corrosion**, 4(2):1-4 .(2018)

34. Ureña, J., et al., "*Corrosion and tribocorrosion behaviour of β-type Ti-Nb and Ti-Mo surfaces designed by diffusion treatments for biomedical applications*". **Corrosion Science**, 140:51-60.(2018)

35. Fowler, L., et al., "*Development of Antibacterial Ti-Cu x Alloys for Dental Applications: Effects of Ageing for Alloys with Up to 10 wt% Cu*". 12(23):4017.(2019)

36. Da Silva, F.L., et al., "*A New Ternary Alloy Ti26Zr24Nb for Biomedical Application: Behavior in Corrosion, Wear, and Tribocorrosion*". **Journal of Bio-and Tribo-Corrosion**, 6(3):1-13.(2020)

37. Mahundla, M., et al., "*Corrosion behaviour of Ti–34Nb–25Zr alloy fabricated by spark plasma sintering*". **Journal of Bio-and Tribo-Corrosion**, 6(2):1-9 .(2020)

38. Çaha, I., et al., "*A Review on Bio-functionalization of β-Ti Alloys*". **Journal of Bio-and Tribo-Corrosion**, 6(4):1-31.(2020)

39. Al-Murshdy, J.M.S., Al-Deen ،H. H. J., & Hussein, S. R, "*Investigation of the Effect of Indium Addition on the Mechanical and Electrochemical Properties of the Ti–15Mo Biomedical Alloy".* **Journal of Bio-and Tribo-Corrosion**, 7(4):1-18.(2021)

40. Shivaram, M.J., Arya, S. B., Nayak, J & ،.Panigrahi, B. B., "*Tribocorrosion behaviour of biomedical porous Ti–20Nb–5Ag alloy in simulated body fluid. ".* **Journal of Bio-and Tribo-Corrosion,** 7(2):1-9.(.(2021)) .

41. Rack, H. and J.J. Qazi, "*Titanium alloys for biomedical applications".* **Materials Science Engineering: C**,26(8):1269-1277 (2006).

42. Smith, W.F.J.M.-H.B.C., xiv+ 512, 23 x 16 cm, illustrated, "*Structure and properties of engineering alloys*.(1981) ."

43. Lütjering, G. and J.C. Williams, *Titanium matrix composites*. 2007: Springer Berlin Heidelberg.

44. Karasevskaya, O., et al., "*Deformation behavior of beta-titanium alloys".* **Materials Science Engineering: A**, 354(1-2)121-132 (2003).

45. Leyens, C. and M. Peters, *Titanium and titanium alloys: fundamentals and applications*. 2003 :John Wiley & Sons.

46. Li, S., et al., "*Ultrafine-grained β-type titanium alloy with nonlinear elasticity and high ductility".* **Applied Physics Letters** , 92(4): 043128 (2008)

47. Banumathy, S., et al., "*Effect of thermomechanical processing on evolution of various phases in Ti-Nb alloys".* **Bulletin of Materials Science**,34(7)1421-1434 (2011).

48. Oliveira, N.T., et al., "*Corrosion resistance of anodic oxides on the Ti–50Zr and Ti–13Nb–13Zr alloys".* **Electrochimica Acta**, 51(10):2068-2075.(2006)

49. Liu, J ،.et al., "*The antibacterial properties and biocompatibility of a Ti–Cu sintered alloy for biomedical application".* **Biomedical Materials**, 9(2):025013.(2014)

50. Donthula, H., et al., "*Morphological evolution of transformation products and eutectoid transformation (s) in a hyper-eutectoid Ti-12 at% Cu alloy".* 168:63-75.(2019)

51. Zhang, E., et al., "*Optimization of mechanical properties, biocorrosion properties and antibacterial properties of as-cast Ti–Cu alloys".* **Biomedical Materials**, 11(6):065001 (2.(016

52. Liu, C. and E.J. Zhang, "*Biocorrosion properties of antibacterial Ti–10Cu sintered alloy in several simulated biological solutions".* **Journal of Materials Science: Materials in Medicine**, 26(3):1-12.(2015)

53. Kumar, K.H., et al., "*Thermodynamic optimisation of the Cu-Ti system"*. **International Journal of Materials Research**, 87(8):666-672.(1996)

54. Li, M., et al., "*Toward a molecular understanding of the antibacterial mechanism of copper-bearing titanium alloys against staphylococcus aureus* ." **Advanced healthcare materials**, 5(5):557-566.(2016)

55. Ke, Z., et al., "*Characterization of a new Ti-13Nb-13Zr-10Cu alloy with enhanced antibacterial activity for biomedical applications"*. **Materials Letters**, 253:335-338.(2019)

56. Ho, W.-F. et al" ،.*Effects of molybdenum content on the structure and mechanical properties of as-cast Ti–10Zr-based alloys for biomedical applications"*. **Materials Science Engineering: C**, 32(2):517-522 (2012).

57. Liu, Y., et al., "*Design of powder metallurgy titanium alloys and composites"*. **Materials Science Engineering: A**,418(1-2):25-35 (2006).

58. Müller, F.A., et al., "*In vitro apatite formation on chemically treated (P/M) Ti–13Nb–13Zr"*. **Dental materials**, 24(1):50-56 (2008).

59. Hasirci, V. and N. Hasirci, *Biomaterials and Devices in Hard Tissue Augmentation*, in *Fundamentals of Biomaterials*. 2018, Springer. p. 219-232.

60. Nouri, A., P.D. Hodgson, and C.J. Wen, "*Effect of ball-milling time on the structural characteristics of biomedical porous Ti–Sn–Nb alloy"*. **Materials Science Engineering: C,**31 (5):921-928 (2011).

61. Breen, D. and D.J. Stoker, "*Titanium lines: a manifestation of metallosis and tissue response to titanium alloy megaprostheses at the knee"*. **Clinical radiology**, 47(4):274-277.(1993)

62. Ananth, H., et al., "*A review on biomaterials in dental implantology"*. 11(3):113.(2015)

63. Niinomi, M., *Metals for biomedical devices*. 2019: Woodhead publishing.

64. Okazaki, Y. and E.J. Gotoh, "*Comparison of fatigue strengths of biocompatible Ti-15Zr-4Nb-4Ta alloy and other titanium materials"*. **Materials Science Engineering: C**,31(2):325-333 (2011).

65. Mohammadi, H. and K.J. Mequanint, "*Prosthetic aortic heart valves: modeling and design"*. **Medical engineering physics**, 33(2):131-147 (2011).

66. Rogers, C. and E.R.J .Edelman, "*Endovascular stent design dictates experimental restenosis and thrombosis"*. **Circulation**, 91(12):2995-3001 .(1995)

67. Winkler, T., et al., "*A review of biomaterials in bone defect healing, remaining shortcomings and future opportunities for bone tissue engineering: The unsolved challenge"*. **Bone joint research**,7(3):232-243 (2018).

68. Gnedenkov, S.V., et al., "*Functional coatings formed on the titanium and magnesium alloys as implant materials by plasma electrolytic oxidation technology: fundamental principles and synthesis conditions*". **Corrosion reviews**, 34(1-2):65-83.(2016)

69. Geetha, M., et al., "*Ti based biomaterials, the ultimate choice for orthopaedic implants–a review*". **Progress in materials science**, 54(3):397-425.(2009)

70. Gepreel, M.A.-H. and M.J. Niinomi, "*Biocompatibility of Ti-alloys for long-term implantation*". **Journal of the mechanical behavior of biomedical materials**, 407:20-415 (2013).

71. Williams, R.J.P.J., "*The natural selection of the chemical elements*". **Cellular Molecular Life Sciences CMLS**, 53(10):816-829 (1997).

72. Quach, N.-C., P.J. Uggowitzer, and P.J. Schmutz, "*Corrosion behaviour of an Mg–Y–RE alloy used in biomedical applications studied by electrochemical techniques*". **Comptes Rendus Chimie**, 11(9):1043-1054.(2008)

73. Koike, M., et al., "*Corrosion behavior of cast titanium with reduced surface reaction layer made by a face-coating method*". **Biomaterials**, 24(25):4541-4549.(2003)

74. Cremasco, A., et al., "*Electrochemical corrosion behavior of a Ti–35Nb alloy for medical prostheses*". **Electrochimica Acta**, 53(14):4867-4874.(2008)

75. Martins, D., et al., "*Solute segregation and its influence on the microstructure and electrochemical behavior of Ti–Nb–Zr alloys*". **Journal of alloys compounds**, 478 (1-2):111-116 (2009).

76. Capela, M.V., et al., "*Repeatability of corrosion parameters for titanium–molybdenum alloys in 0.9% NaCl solution*". 465(1-2):479-483.(2008)

77. Oliveira, N.T., et al., "*Development of Ti–Mo alloys for biomedical applications: Microstructure and electrochemical characterization*". **Materials Science Engineering: A**, 727:425-731 (2007).

78. Metikoš-Huković, M. et al., "*An in vitro study of Ti and Ti-alloys coated withsol–gel derived hydroxyapatite coatings*". **Surface Coatings Technology**,165 (1): 40-50 (2003).

79. Fowler, L., *Development of titanium-copper alloys for dental applications*. 2019, Acta Universitatis Upsaliensis.

80. Park, H.-S., T.-G. Kwon, and O.-W.J. Kwon, "*Treatment of open bite with microscrew implant anchorage*". **American journal of orthodontics dentofacial orthopedics**, 126(5):627-636 (2004).

81. Putters, J., et al., "*Comparative cell culture effects of shape memory metal (Nitinol®), nickel and titanium: a biocompatibility estimation*". **European surgical research** , 24(6):378-282(1992).

82. Coogan, T.P., et al., "*Toxicity and carcinogenicity of nickel compounds"*. **CRC Critical reviews in toxicology**, 19(4):341-384.(1989)

83. He, G. and M.J. Hagiwara, "*Ti alloy design strategy for biomedical applications"*. **Materials Science Engineering: C**,26 (1):14-19 (2006).

84. Hattori, T., et al., "*Material rigidity of fracture fixation device and bone tissue reaction—experimantal study on intramedullary fixation with different materials"*. **J. Jpn Clin. Biomech**, 23:299-304.(2002)

85. Ning, C., et al., "*The effect of Zr content on the microstructure, mechanical properties and cell attachment of Ti–35Nb–xZr alloys"*. **Biomedical Materials**, 5(4):045006.(2010)

86. German, R.M.J., "*Powder metallurgy science"*. **Metal Powder Industries Federation**:279 (19.(84

87. Ng, H.P. et al., "*Improving sinterability of Ti–6Al–4V from blended elemental powders through equal channel angular pressing"*. **Materials Science Engineering: A**,396:404-565 (2013).

88. Silva, A.G.P.d., and C.J. Alves Júnior, "*Rapid sintering: its application, analysis, and relation with the innovative sintering techniques"*. **Cerâmica**, 44:225-232.(1998)

89. Blanco, E., H. Shen, and M.J. Ferrari, "*Principles of nanoparticle design for overcoming biological barriers to drug delivery"*. **Nature Biotechnology**, 33(9):941-951.(2015)

90. German, R., *Thermodynamics of sintering*, in *Sintering of advanced materials*. 2010, Elsevier. p. 3-32.

91. Groover, M.P., *Fundamentals of modern manufacturing: materials, processes, and systems*. 2020: John Wiley & Sons.

92. Al-Qudsi, A., et al., "*Comparison between different numerical models of densification during solid-state sintering of pure aluminium powder"*. **Production Engineering**, 9(1):11-24.(2015)

93. Yong, A.P., M.A. Islam, and N.J. Hasan, "*A review: Effect of pressure on homogenization"*. **Sigma Journal of Engineering Natural Sciences**,35(1):1-22 (2017).

94. Severino Martins Jr, J.R. and C.R.J. Grandini, "*Structural characterization of Ti-15Mo alloy used as biomaterial by Rietveld method"*. **Journal of Applied Physics**, 111(8):083535.(2012)

95. Dass, K., S. Chauhan, and B.J. Gaur, "*Study on mechanical and dry sliding wear characteristics of meta-cresol Novalac epoxy composites filled with silicon carbide, aluminum oxide, and zinc oxide particulates"*. **Tribology Transactions**, 57(2):157-172.(2014)

96. Rasool, G., Y. El Shafei, and M.M.J. Stack, "*Mapping tribo-corrosion behaviour of TI-6AL-4V Eli in laboratory simulated hip joint environments*". **Lubricants**, 8(7):69.(2020)

97. Yılmaz, E., et al., "*Characterization of biomedical Ti-16Nb-(0–4) Sn alloys produced by powder injection molding*". **Vacuum**, 142:164-174.(2017)

98. Sato, K., M. Takahashi, and Y.J. Takada, "*Construction of Ti-Nb-Ti2Cu pseudo-ternary phase diagram*". **Dental materials journal**, 39(3):422-428 (202.(0

99. Henriques, V.A.R., et al. *Microstructural evolution of Ti-13Nb-13Zr alloy during sintering*. in *Materials science forum*. 2005. Trans Tech Publ.

100. Martins, G., et al. *Microstructural evolution of Ti-10Nb and Ti-15Nb alloys produced by the blended elemental technique*. in *Materials Science Forum*. 2010. Trans Tech Publ.

101. Zhao, D., et al., "*Sintering behavior and mechanical properties of a metal injection molded Ti–Nb binary alloy as biomaterial*". **Journal of Alloys Compounds**, 393:400-640 (2015).

102. Yi, C., et al., "*Antibacterial Ti-Cu alloy with enhanced mechanical properties as implant applications*". **Materials Research Express**,7(10): 105404 (2020).

103. Vlcak, P., et al., "*Surface pre-treatments of Ti-Nb-Zr-Ta beta titanium alloy: The effect of chemical, electrochemical and ion sputter etching on morphology, residual stress, corrosion stability and the MG-63 cell response*". **Results in Physics**, 28:104613.(2021)

104. Cheng, H.-C., et al., "*Biomechanical research of TiNb alloys with electrochemical treatment using finite element method*". **ECS Transactions**, 13(7):1.(2008)

105. Dong, W., P. Sullivan, and K.J. Stout, "*Comprehensive study of parameters for characterising three-dimensional surface topography: III: Parameters for characterising amplitude and some functional properties*". **Wear**, 178(1-2):29-43.(1994)

106. Stamboliska, Z. and M. Kuzinovski, "*Analysis and Mathematical Interpretation of Parameters That Describe the Microstereometry of Machined Surfaces*". **J JOURNAL-BALKAN TRIBOLOGICAL ASSOCIATION**, 5(3/4):223-231.(1999)

107. Kjeldsteen, P. *Wear resistance of PM materials and its dependency on surface topography*. in *Powder Metallurgy World Congress(PM'94)*. 1994.

108. Kjeldsteen, P., *Tribological investigations of P/M Stainless steels mixed with HCX23 against Al2O3 & SiC*. 1997, Danfoss Research Report MUP2.

109. Kikuchi, M., et al., "*Mechanical properties and microstructures of cast Ti–Cu alloys"*. **Dental materials**, 19(3):174-181.(2003)

110. Mutlu, I., S. Yeniyol, and E.J. Oktay, "*Production and Precipitation Hardening of Beta-Type Ti-35Nb-10Cu Alloy Foam for Implant Applications"*. **Journal of Materials Engineering Performance**, 25 (4): 1586-1593 (2016).

111. Wang, Y. and Y.J. Zheng, "*Corrosion behaviour and biocompatibility evaluation of low modulus Ti–16Nb shape memory alloy as potential biomaterial"*. **Materials Letters**,63(15):1293-1295 (2009).

112. Mutlu, I. and E.J. Oktay, "*Localised corrosion behaviour of biomedical implant materials using electrochemical potentiokinetic reactivation and critical pitting potential methods"*. **Corrosion Engineering, Science Technology**,50 (1):72-79 (2015).

113. Hikmat, N.A., A.M. Farhan, and R.A.J. Majed, "*Effect of Chloride Ions on the Passive Layer for Three Al-alloys at pH= 9"*. **Al-Nahrain Journal of Science**, 12(3):23-32 (2009).

114. Daroonparvar, M. et al., "*Modification of surface hardness, wear resistance and corrosion resistance of cold spray Al coated AZ31B Mg alloy using cold spray double layered Ta/Ti coating in 3.5 wt% NaCl solution"*. 176:109029.(2020)

115. Zhang, E., et al., "*A new antibacterial titanium–copper sintered alloy: preparation and antibacterial property"*. **Materials Science Engineering: C**, 33(7):4280-4287 (2013).

116. Wang, X. et al., "*In vivo antibacterial property of Ti-Cu sintered alloy implant"*. **Materials Science Engineering: C**,38:47-100 (2019).

117. Javadhesari, S.M., S. Alipour, and M.J. Akbarpour, "*Biocompatibility, osseointegration, antibacterial and mechanical properties of nanocrystalline Ti-Cu alloy as a new orthopedic material"*. **Colloids Surfaces B: Biointerfaces**, 110889:189 (2020).

118. Javadhesari, S.M., S. Alipour, and M.J. Akbarpour, "*Effects of SiC nanoparticles on synthesis and antimicrobial activity of TiCu nanocrystalline powder"*. **Ceramics International**, 46.(2020) 120-114:(1)

119. Cabiscol Català, E., J. Tamarit Sumalla, and J. Ros Salvador, "*Oxidative stress in bacteria and protein damage by reactive oxygen species"*. **International Microbiology**, 3(1):3-8.(2000)

CURRICULUM VITAE

Mohammed Riyadh Abdulameer ALAAWAD is a material engineer who graduated from the Faculty of Engineering, University of Technology - Iraq. He received His Bachelor’s degree in 2003. He is currently studying for her Master's degree at Karabük University in the field of Materials Engineering.